BRIGHAM YOUNG UNIVERSITY

GEOLOGY STUDIES

GEOLOGICAL SOCIETY OF AMERICA

FIELD TRIP GUIDE BOOK

1997 ANNUAL MEETING • SALT LAKE CITY, UTAH

PART TWO

EDITED BY PAUL KARL LINK AND BART J. KOWALLIS

VOLUME 42 • 1997

MESOZOIC TO RECENT GEOLOGY OF UTAH

Edited by

Paul Karl Link and Bart J. Kowallis

BRIGHAM YOUNG UNIVERSITY
GEOLOGY STUDIES
Volume 42, Part II, 1997

CONTENTS

A Publication of the
Department of Geology
Brigham Young University
Provo, Utah 84602

Brigham Young University Geology Studies is published by the Department of Geology. This publication consists of graduate student and faculty research within the department as well as papers submitted by outside contributors. Each article submitted is externally reviewed by at least two qualified persons.

Cover photos taken by Paul Karl Link.

Top: Upheaval Dome, southeastern Utah.

Middle: Lake Bonneville shorelines west of Brigham City, Utah.

Bottom: Bryce Canyon National Park, Utah.

ISSN 0068-1016
9-97 700 23870/24290

Preface

Guidebooks have been part of the exploration of the American West since Oregon Trail days. Geologic guidebooks with maps and photographs are an especially graphic tool for school teachers, University classes, and visiting geologists to become familiar with the territory, the geologic issues and the available references.

It was in this spirit that we set out to compile this two-volume set of field trip descriptions for the Annual Meeting of the Geological Society of America in Salt Lake City in October 1997. We were seeking to produce a quality product, with fully peer-reviewed papers, and user-friendly field trip logs. We found we were bucking a tide in our profession which de-emphasizes guidebooks and paper products. If this tide continues we wish to be on record as producing "The Last Best Geologic Guidebook."

We thank all the authors who met our strict deadlines and contributed this outstanding set of papers. We hope this work will stand for years to come as a lasting introduction to the complex geology of the Colorado Plateau, Basin and Range, Wasatch Front, and Snake River Plain in the vicinity of Salt Lake City. Index maps to the field trips contained in each volume are on the back covers.

Part 1 "Proterozoic to Recent Stratigraphy, Tectonics and Volcanology: Utah, Nevada, Southern Idaho and Central Mexico" contains a number of papers of exceptional interest for their geologic synthesis. Part 2 "Mesozoic to Recent Geology of Utah" concentrates on the Colorado Plateau and the Wasatch Front.

Paul Link read all the papers and coordinated the review process. Bart Kowallis copy edited the manuscripts and coordinated the publication via Brigham Young University Geology Studies. We would like to thank all the reviewers, who were generally prompt and helpful in meeting our tight schedule. These included: Lee Allison, Genevieve Atwood, Gary Axen, Jim Beget, Myron Best, David Bice, Phyllis Camilleri, Marjorie Chan, Nick Christie-Blick, Gary Christenson, Dan Chure, Mary Droser, Ernie Duebendorfer, Tony Ekdale, Todd Ehlers, Ben Everitt, Geoff Freethey, Hugh Hurlow, Jim Garrison, Denny Geist, Jeff Geslin, Ron Greeley, Gus Gustason, Bill Hackett, Kimm Harty, Grant Heiken, Lehi Hintze, Peter Huntoon, Peter Isaacson, Jeff Keaton, Keith Ketner, Guy King, Mel Kuntz, Tim Lawton, Spencer Lucas, Lon McCarley, Meghan Miller, Gautam Mitra, Kathy Nichols, Robert Q. Oaks, Susan Olig, Jack Oviatt, Bill Perry, Andy Pulham, Dick Robison, Rube Ross, Rich Schweickert, Peter Sheehan, Norm Silberling, Dick Smith, Barry Solomon, K.O. Stanley, Kevin Stewart, Wanda Taylor, Glenn Thackray and Adolph Yonkee. In addition, we wish to thank all the dedicated workers at Brigham Young University Print Services and in the Department of Geology who contributed many long hours of work to these volumes.

Paul Karl Link and Bart J. Kowallis, Editors

Extensional Faulting, Footwall Deformation and Plutonism in the Mineral Mountains, Southern Sevier Desert

DREW S. COLEMAN
Department of Earth Sciences, 675 Commonwealth Avenue, Boston University, Boston, Massachusetts 02215

JOHN M. BARTLEY
Department of Geology and Geophysics, 717 WBB, University of Utah, Salt Lake City, Utah 84112

J. DOUGLAS WALKER
Department of Geology, 120 Lindley Hall, University of Kansas, Lawrence, Kansas 66045

DAVID E. PRICE
Department of Geology and Geophysics, 717 WBB, University of Utah, Salt Lake City, Utah 84112

ANKE M. FRIEDRICH
Department of Earth, Atmospheric and Planetary Sciences, Massachusetts Institute of Technology, 54-1118, Cambridge, Massachusetts 02139

ABSTRACT

Structural relations in the Mineral Mountains and surrounding area in southern Utah indicate that the major north-south striking Cenozoic normal faults in the region were tilted to their present gentle dips by either rolling-hinge style footwall uplift or domino style faulting. Field, geochronologic and thermochronologic data demonstrate that the main period of east-west directed extension along these normal faults occurred 6 to 7 Ma after peak magmatism. Thus, no direct link between magmatism, normal faulting and ductile deformation associated with normal faulting exists in the area. Prior to, and synchronous with, the main episode of east-west directed extension, several sets of northeast- to northwest-striking normal faults generated a series of east-west trending grabens throughout the region. The timing of formation of these grabens varies across the study area and overlaps with regional magmatism. We infer a large amount of slip along the Sevier Desert detachment fault which is the only structure north of the Mineral Mountains that could accommodate the extensional deformation documented there. This argues against the interpretation that the Sevier Desert reflector is the result of fortuitous alignment of a Mesozoic thrust fault and a Cenozoic unconformity. Tertiary extension disrupted Mesozoic thrust faults across the Mineral Mountains and surrounding ranges; however, new mapping provides a basis for regional correlation. We correlate the Wah Wah, Frisco and Antelope Mountain thrusts, and a sub-Antelope Mountain thrust with the Beaver Lake thrust and Dry Canyon/Tetons thrust zone.

INTRODUCTION

The common spatial and temporal association of magmatism and metamorphic core complexes suggests that a genetic relation exists between the two. The association of broadly coeval plutonic rocks with low-angle mylonitic detachment faults led Gans (1987), Lister and Baldwin (1993) and Parsons and Thompson (1993) to suggest direct links between magmatism, ductile deformation in core complexes, and the development of low-angle normal faults. In contrast, Axen et al., (1993) and Coleman et al., (in preparation) acknowledge the widespread importance of magmatism in extension, but find no consistent temporal or genetic link between magmatism and formation of extensional core complexes.

Another persistent debate regarding the origin of extensional core complexes is whether presently low-angle normal faults were active with shallow dips (e.g., Wernicke, 1981; Davis and Lister, 1988; Reynolds and Lister, 1990; Scott and Lister, 1992), or were active as moderately to steeply dipping normal faults that were subsequently tilted to shallow orientations (Proffett, 1977; Buck, 1988; Wernicke and Axen, 1988). Evaluating footwall deformation is difficult in core complexes that are dominated by young plutonic rocks that lack markers for reconstruction of structural geometries (e.g., Reynolds and Rehrig, 1980; Gans, 1987; Walker et al., 1990; Lister and Baldwin, 1993; Wright and Snoke, 1993; Coleman and Walker, 1994). The nature and amount of footwall deformation in such complexes has been examined indirectly using paleomagnetic and/or thermochronologic data (Holm et al., 1990; Hoisch and Simpson, 1993; John and Foster, 1993; Livaccari et al., 1993, 1995; Coleman and Walker, 1994; Coleman et al., in preparation). Furthermore, structures that directly record rebound kinematics in initially isotropic plutonic rocks are increasingly recognized (Bartley et al., 1990; Manning and Bartley, 1994; Axen et al., 1995).

The debate regarding the original orientation of low-angle detachment faults recently took on new life with the assertion that the reflector in west central Utah, previously interpreted as the Sevier Desert extensional detachment (MacDonald, 1976; Allmendinger et al., 1983; Von Tish et al., 1985), actually is defined by the coincidental alignment of a Mesozoic thrust fault and the sub-Tertiary unconformity (Anders and Christie-Blick, 1994). The Mineral Mountains in southwest Utah lie directly south of the Sevier Desert, and displacement across the Sevier Desert detachment is interpreted to be partially accommodated in this and adjacent basins and ranges (figs. 1 and 2; Price and Bartley, 1990; Coleman, 1991; Coleman and Walker, 1994; Price, in preparation). The Tertiary Mineral Mountains batholith, which forms the majority of the northern and central part of the range (Smith and Bruhn, 1984; Nielson et al., 1986; Coleman, 1991; Coleman and Walker, 1992), lies in the footwall of the Cave Canyon detachment. The detachment and a klippe of its hanging wall are preserved in the southern part of the range (Nielson et al., 1986; Price and Bartley, 1990, 1992; Price, in preparation). The structural geology, petrology, geochronology and paleomagnetism of the Mineral Mountains and ranges to the west reveal the history of the Cave Canyon detachment and related faults, and provide insight into the amount and nature of crustal extension southward along strike from the Sevier Desert.

The principal aim of this trip is to examine what we have learned regarding the relationship between magmatism and extension in the Mineral Mountains. We will also examine field data bearing on the nature of footwall deformation and the amount of extension accommodated in the area. We present relevant results of field work in the Mineral Mountains and nearby Star Range, Beaver Lake Mountains and Wah Wah Mountains (figs. 1 and 2). We show evidence that magmatism and extension were not synchronous, but rather, that the main pulse of plutonism ended at least 6 Ma before the Cave Canyon detachment exhumed the plutonic complex (Coleman et al., in preparation). Furthermore, closely following the last episode of intrusive magmatism, unroofing of the plutonic complex by slip across the Cave Canyon detachment resulted in up to 90° of west-side-up tilting resulting in the present low-angle geometry of the fault (Price and Bartley, 1990, 1992; Coleman and Walker, 1994; Coleman et al., in preparation; Price, in preparation). Finally, restoration of mapped regional normal faults accounts for a minimum of 20 kilometers of east-west directed extension. Because no other structures that could accommodate this magnitude of slip are recognized to the north, these observations support the existence of, and large slip across, the Sevier Desert detachment.

An additional focus of our work in the Mineral Mountains region has been to document structural relations of the thrust faults in the area, including their overprinting by Cenozoic deformation, and to correlate the isolated exposures from range to range. Although severely disrupted by Tertiary extension, several thrust faults of regional significance are exposed in the area (figs. 1 and 2), including the Beaver Lake, Antelope Mountain, Pavant, and Frisco/Wah Wah thrusts. One of the aims of the field trip is to examine possible correlations amongst these structures.

MAP UNITS

Proterozoic Basement

Precambrian banded gneiss crops out on the western margin of the Mineral Mountains batholith (fig. 2, unit pC; Stop 1-5; Nielson et al., 1978; Sibbett and Nielson, 1980). Aleinikoff et al., (1987) report a U-Pb zircon age of 1716 ± 31 Ma and a Rb/Sr model age of 1750 Ma for the gneiss.

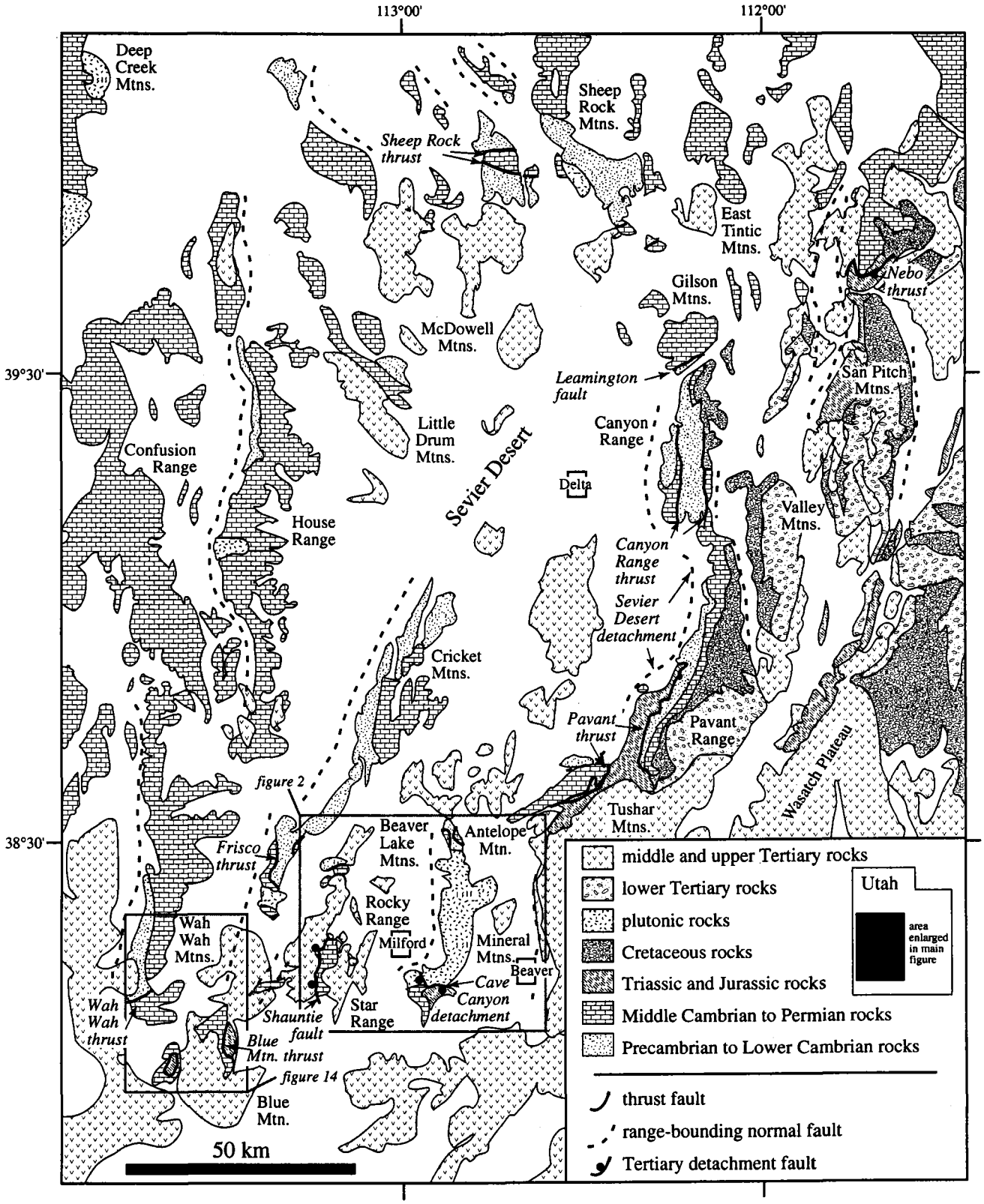

Figure 1. Simplified geologic map of southwestern Utah simplified after Hintze (1980) showing major thrust, normal and detachment faults. Locations of figures showing greater detail of the geology are also shown.

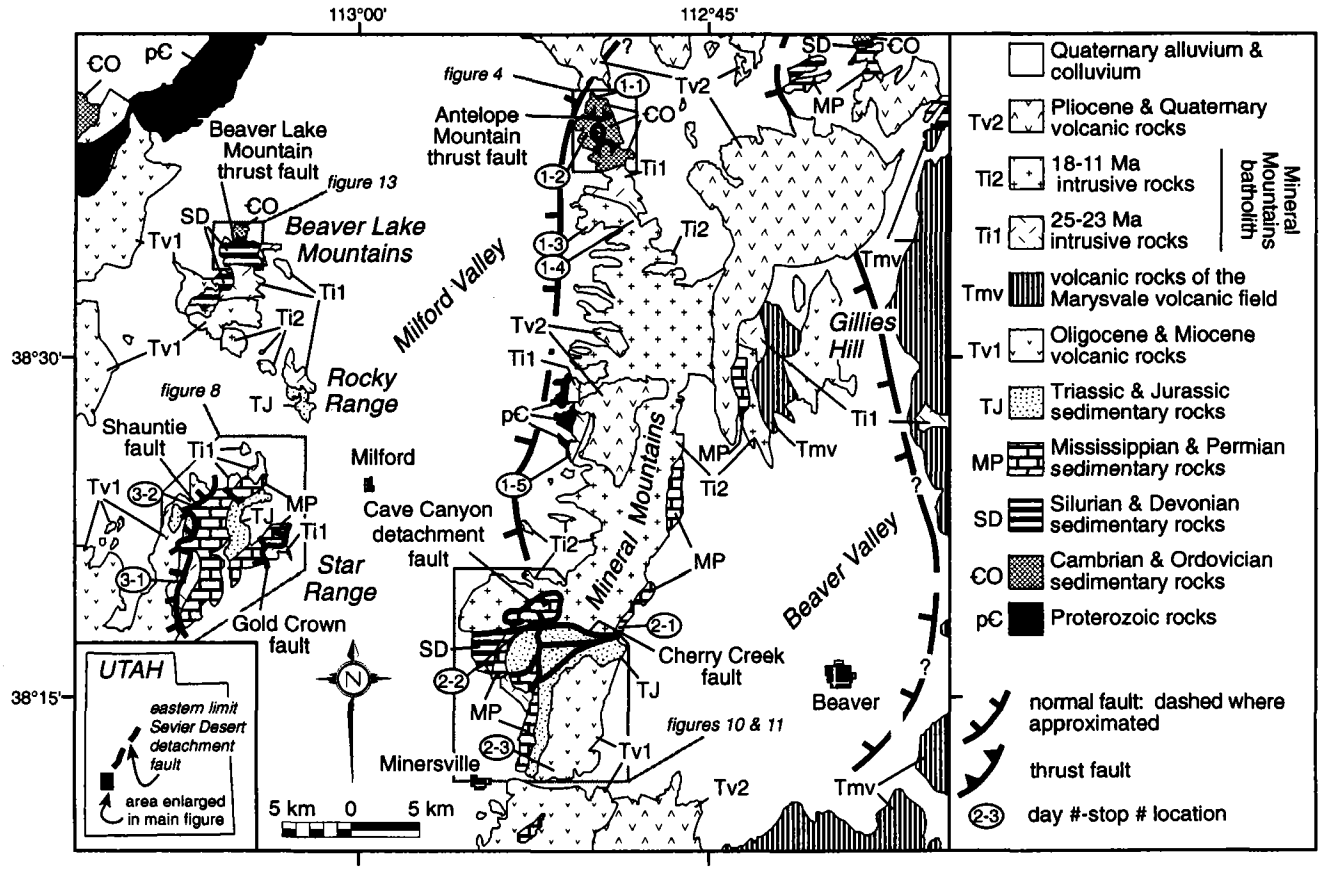

Figure 2. Simplified geologic map of the Mineral Mountains and surrounding ranges. Approximate field trip stop locations and areas of more detailed geologic map figures are shown. Geologic data from Hintze (1980), Coleman (1991), Price (in preparation) and this study. Modified after Coleman and Walker (1992).

Quartzite containing minor biotite, feldspar and chlorite occurs as inclusions within the Precambrian biotite gneiss and as xenoliths in the Mineral Mountains batholith (Nielson et al., 1978; Sibbett and Nielson, 1980; Coleman, 1991). Thin layers of sillimanite-K-feldspar schist also are found as inclusions in the batholith near exposures of the Precambrian biotite gneiss (Nielson et al., 1978; Sibbett and Nielson, 1980; Coleman, 1991). The quartzite and schist are assigned a Precambrian age because of their close association with the gneiss and high metamorphic grade; no known exposed Paleozoic wallrock experienced sillimanite zone metamorphism. Nielson et al., (1978) and Sibbett and Nielson (1980) interpreted the gneiss as a paragneiss on the basis of its field relations with the sillimanite schist and quartzite and the nature of banding within the unit.

Paleozoic-Mesozoic Rocks

Late Proterozoic to Mesozoic strata in the Mineral Mountains region represent the transition from the miogeocline to the craton inboard of a west-facing continental margin (fig. 3). The area lies outside of the late Paleozoic Oquirrh basin of northern Utah and is sufficiently far from the ancient continental margin not to have recorded the Antler or Sonoma orogenies. It thus was tectonically quiescent from late Proterozoic time until initiation of the Sevier orogeny in latest Jurassic to early Cretaceous time when continental-margin facies were stacked, telescoped, and thrust toward the craton (Armstrong and Oriel, 1965; Armstrong, 1968; Heller et al., 1986; Royse, 1993; DeCelles et al., 1995).

Antelope Mountain

Stratified rocks of Cambrian and Cretaceous(?) age are exposed on Antelope Mountain at the northern end of the Mineral Mountains (fig. 2, unit CO; fig 4; Stops 1-1 and 1-2). Cambrian strata are part of the miogeoclinal sequence that is well described elsewhere (Hintze and Robison, 1975). Conglomerate of probable Cretaceous age, unrecognized prior to our mapping, is exposed in three outcrop areas bounded by faults and unconformities (fig. 4; Stop 1-2;

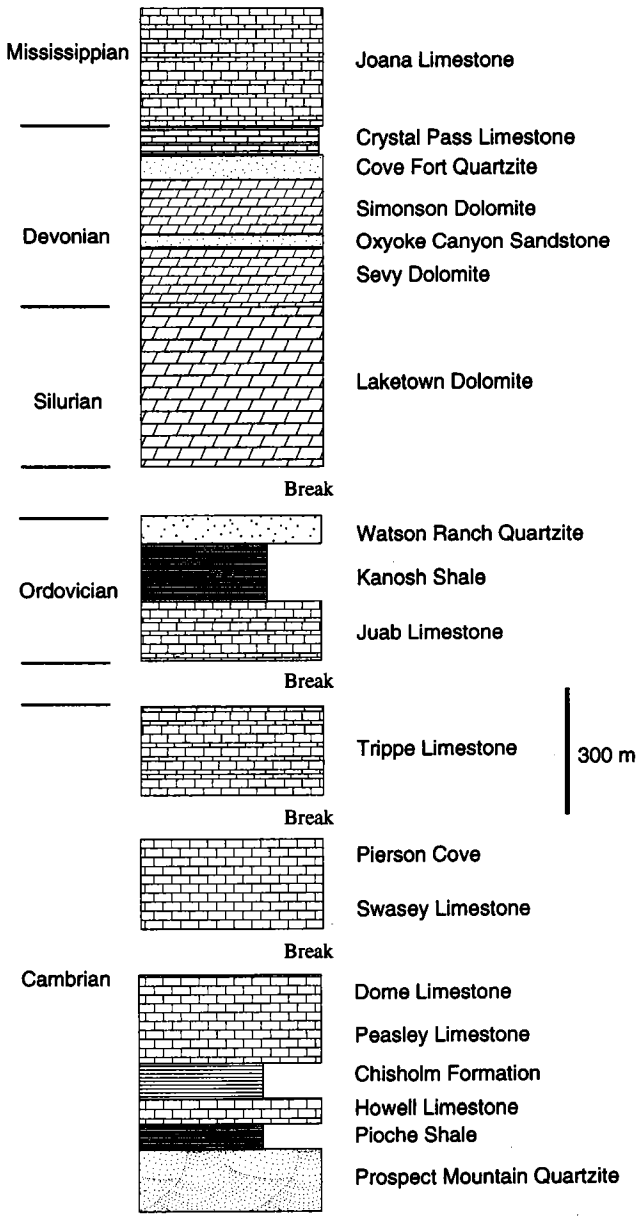

Figure 3. Generalized stratigraphic column for the Beaver Lake and Antelope Mountain areas. Unit assignments after Hintze and Robison (1975), Barosh (1960), and Lemmon and Morris (1984). Breaks in section correspond with faults within and between the two areas.

Walker and Bartley, 1991). The rocks consist of unfossiliferous, orange-weathering calcareous siltstone and conglomerate with subordinate quartz sandstone. Siltstone beds are typically thinly laminated (1 mm) and from 0.5 to 1 meter thick. Conglomerate beds are thick (1 to 5 m) and massively stratified. The conglomerate is mostly matrix-supported and the matrix consists of orange-weathering siltstone. Clasts include quartzite and carbonate rocks identical to Cambrian strata in the hanging wall and footwall of the Antelope Mountain thrust. The basal contact of the conglomerate is an unconformity developed on progressively older Cambrian strata passing to the north. The upper contact is the Antelope Mountain thrust. We correlate these strata with the Cretaceous Indianola Group on the basis of their structural position and lithologic similarity to strata in the southern Pavant Range.

Central Mineral Mountains

Paleozoic rocks exposed in the central Mineral Mountains include recrystallized limestone and dolomite, and quartzite (fig. 2, unit MP; Crawford and Buranek, 1945; Earl, 1957; Condie, 1960; Nielson et al., 1978; Sibbett and Nielson, 1980; Coleman, 1991). Paleozoic sedimentary rocks immediately adjacent to the batholith are generally too metamorphosed to make definitive stratigraphic assignments; however, several workers have assigned ages and/or formation names to various parts of these metasedimentary rocks, and the reader is referred to the references cited above for more detailed descriptions.

Recognizable Paleozoic carbonate wallrocks in the Mineral Mountains include Mississippian Redwall Limestone and a dark colored dolomite that may be correlative with the Devonian Simonson Dolomite on the eastern side of the range (fig. 2; Stop 2-1; Crawford and Buranek, 1945; Sibbett and Nielson, 1980; Price, in preparation), and Permian Kaibab Limestone (Earl, 1957) on the western side. However, Sibbett and Nielson (1980) noted that the carbonate rocks on the western side of the batholith lack the chert nodules characteristic of the Kaibab Limestone, placing some doubt on the correlation made by Earl (1957).

Brown to gray schistose quartzite occurs as inclusions on the eastern side of the Mineral Mountains batholith, and in fault and depositional(?) contact with the carbonate rocks on the western side of the range (Nielson et al., 1978; Sibbett and Nielson, 1980; Coleman, 1991). This rock unit is assigned a Paleozoic age on the basis of the interpreted stratigraphic contact with rocks correlated with the Redwall Limestone (Crawford and Buranek, 1945; Nielson et al., 1978; Sibbett and Nielson, 1980) and may be equivalent to the Devonian Cove Fort Quartzite.

Southern Mineral Mountains and Star Range

Stratigraphic sections of pre-Cenozoic rocks exposed in the southern Mineral Mountains and in the Star Range across Milford Valley to the west are similar and therefore are treated together here (fig. 2, units SD, MP and TJ; fig. 5). The oldest exposed strata are assigned to the Devonian Simonson Dolomite based on the characteristic dark color and stromatoporoid fauna. The base of the section is everywhere either faulted, intruded, or concealed. The youngest pre-Cenozoic strata in the Star Range are assigned to the

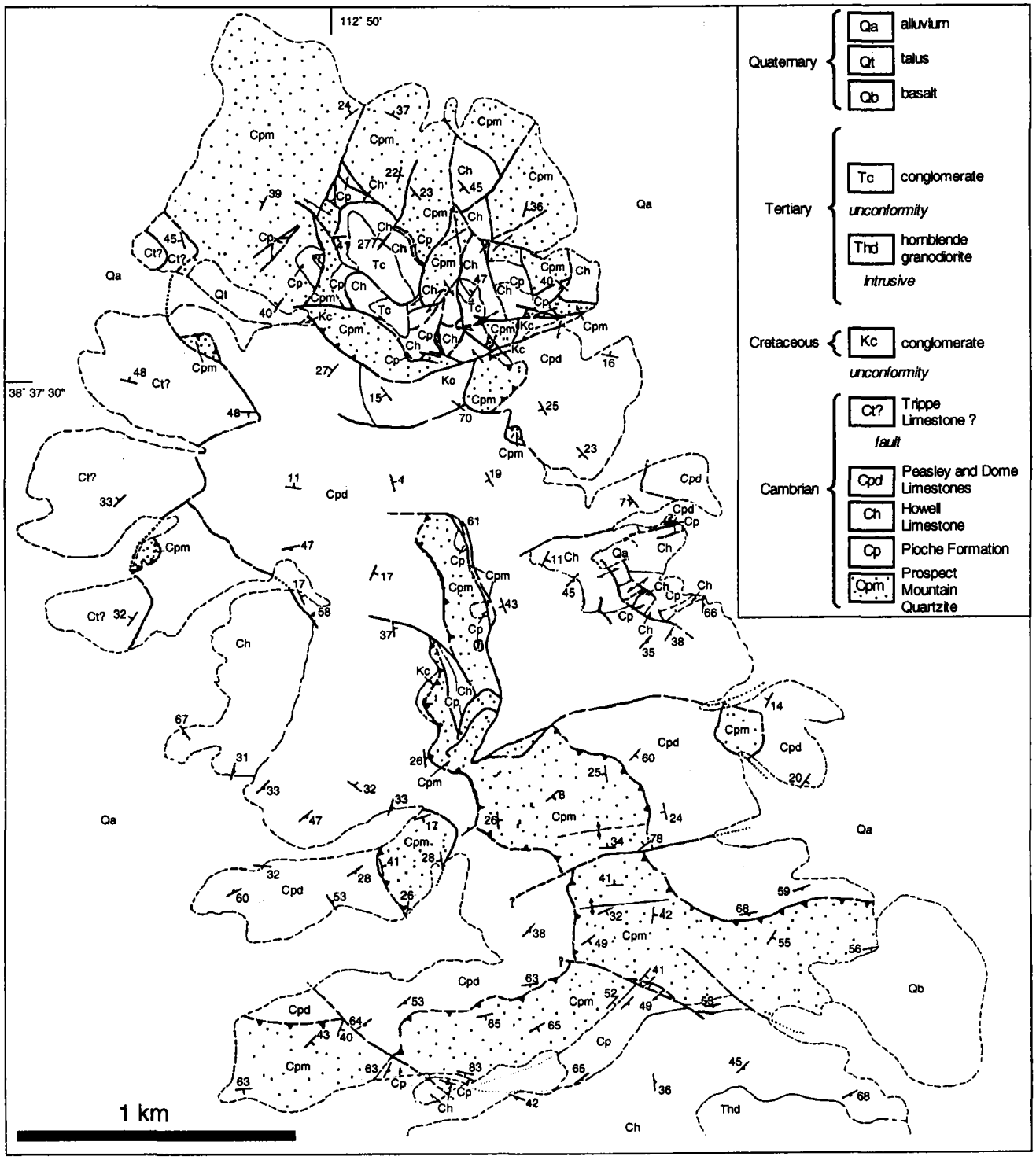

Figure 4. Geologic map of the Antelope Mountain area. The principal structure in this area is the Antelope Mountain thrust (see text for discussion). East-west trending folds in the footwall to the southern section of the Antelope Mountain thrust fault are attributed to synplutonic deformation. Mapping by J.D. Walker and J.M. Bartley.

Jurassic Navajo Sandstone, whereas the Mineral Mountains section locally includes overlying limestone assigned to the Jurassic Carmel Formation. The intervening upper Paleozoic through Triassic section is relatively thin and contains a larger proportion of quartzose clastic rocks and dolostone than miogeoclinal sections. As a result of this relatively cratonal character, most mapped formations are more readily correlated to the Colorado Plateau than to miogeoclinal sections (fig. 5 and compare to fig. 6).

Northern Beaver Lake Mountains

Stratified rocks of Cambrian to Mississippian age are present in the Beaver Lake Mountains (fig. 2 units CO and SD; fig. 3). The rocks are involved in a complex imbricate zone associated with the Beaver Lake thrust, intruded by mid-Tertiary granitoids, and dissected by normal faults; therefore the stratigraphy is fragmentary at best. Stratigraphic nomenclature that has been used for these rocks is a somewhat confusing patchwork of local names and names imported from Nevada and other parts of Utah. We have not attempted to resolve these problems, but use the unit designations of previous workers and names from the Wah Wah Mountains and southern Pavant Range (Barosh, 1960; Hintze, 1974; Abbott et al., 1983; Lemmon and Morris, 1984).

Southern Wah Wah Mountains

Late Proterozoic to Mesozoic strata are exposed as several inliers within the southern Wah Wah Mountains (figs. 6 and 7). Late Proterozoic strata consist mainly of quartzite and occur only in the Wah Wah thrust plate. Cambrian carbonate rocks of the Blue Mountain thrust plate include Upper Cambrian units that are not exposed elsewhere in the Mineral Mountains region. Ordovician to Mississippian carbonate strata are well exposed in several imbricate thrust slices; this section is similar to the section of the Beaver Lake Mountains with the exception of the Oxyoke Canyon Sandstone, which appears as a thin yellow siltstone layer. The upper part of the Mississippian section includes clastic sedimentary rocks that may represent the distal edge of the Antler foreland basin, which is otherwise unrecognized in rocks structurally below the Wah Wah-Canyon Range thrust plate. A relatively complete section of Middle Paleozoic rocks is only preserved in one of the thrust slices (Dry Canyon I thrust plate, Friedrich 1993; figs. 6 and 7). Individual sections appear to be thicker in this area than correlative strata in the Milford Valley area, consistent with a more open miogeoclinal setting.

Cenozoic Rocks

Volcanic Rocks

Tertiary volcanic rocks crop out throughout the Mineral Mountains (figs. 2 and 5; Stop 2-3). At the southern end of the range the sequence includes Oligocene intermediate lava flows assigned to the andesite of the Shauntie Hills, ash-flow tuffs of the Oligocene Needles Range Group (fig. 2, unit Tv1; Best et al., 1989a), and latest Oligocene and early Miocene ash-flow tuffs and near-vent lava flows and volcaniclastic rocks of the Marysvale Volcanic Field (fig. 2, unit Tmv; Bullion Canyon Volcanics and Mt. Dutton Formation; Steven et al., 1979). The andesite of the Shauntie Hills was correlated by Best and Grant (1987) with andesite in the Escalante Desert Formation of the Needles Range Group that has a stratigraphically bracketed age of 34–31 Ma. The youngest volcanic rocks exposed in the southern Mineral Mountains are 7.6 Ma basalt (Best et al., 1980)

On the northeast side of the Mineral Mountains, the Gillies Hill rhyolite was deposited at approximately 9 Ma (fig. 2, unit Tv2; Evans and Steven, 1982), and on the west side of the range, the Corral Canyon rhyolite was deposited at approximately 8 Ma (Evans and Nash, 1978). Quaternary volcanic rocks occur throughout the Mineral Mountains (Nash, 1976; Nielson et al., 1978; Sibbett and Nielson, 1980; Crecraft et al., 1981; Nash and Crecraft, 1982). These rocks include ash-flow tuffs and obsidian lava flows in the central Mineral Mountains that were deposited contemporaneously with basalt lava flows in the northern Mineral Mountains between 0.8 and 0.5 Ma (fig. 2, unit Tv2; Lipman et al., 1978).

Volcanic rocks in the Star Range and Beaver Lake Mountains are Needles Range Group intermediate lavas assigned to the andesite of the Shauntie Hills and to the Horn Silver Andesite (fig. 2, unit Tv1; Stop 3-1; fig. 5). The volcanic section in the Wah Wah Mountains consists mainly of the Needles Range Group, and the bimodal early Miocene Blawn Formation (fig. 6).

Intrusive Rocks

Mineral Mountains. The largest area of the Mineral Mountains exposes a Tertiary batholith intruded between 25 and 11 Ma (Aleinikoff et al., 1987; Coleman and Walker, 1992). During this interval, there were three distinct episodes of magmatism, all characterized by coeval intrusion and mixing of mafic and felsic magmas (Coleman, 1991; Coleman and Walker, 1992; Coleman et al., in preparation). The first is preserved as mixed diorite and hornblende granodiorite (fig. 2, unit Ti1; Coleman, 1991). The second intrusive episode includes rocks ranging in composition from gabbro to high-silica granite and accounts for greater than 90% of the exposed batholith (fig. 2, unit Ti2). The final intrusive episode recorded is emplacement of rhyolite, basalt and mixed rhyolite-basalt dikes at 11 Ma (fig. 2, unit Ti2).

The northern and westernmost parts of the Mineral Mountains batholith comprise an Oligocene [U-Pb zircon age of 25 ± 4 Ma; (Aleinikoff et al., 1987)] resistant, light-

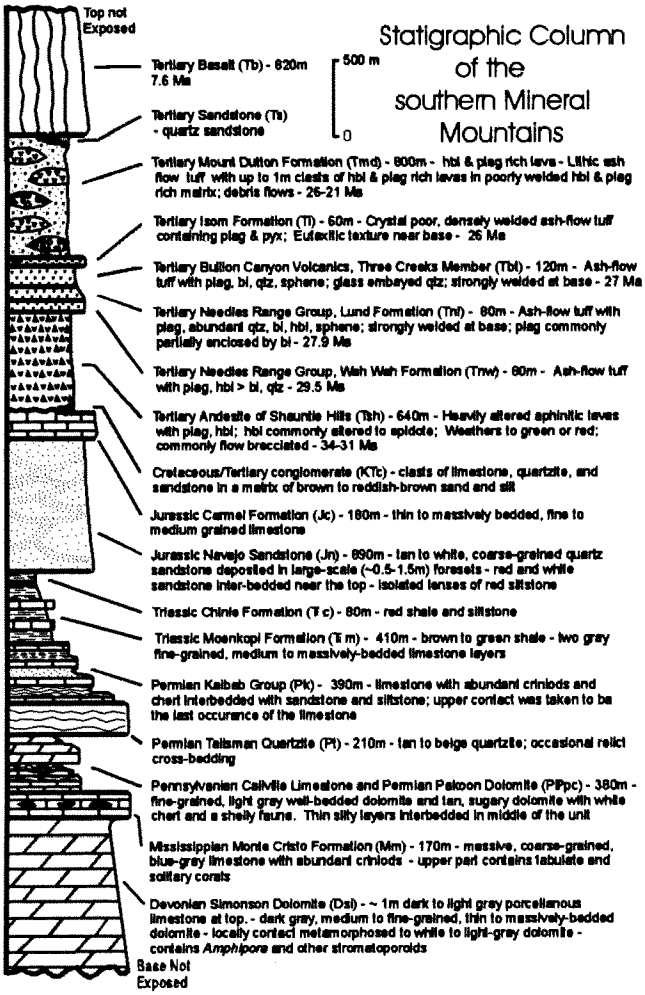

Figure 5. Stratigraphic column for the southern Mineral Mountains. Unit thicknesses (in parentheses) are taken from cross-sections (for example, fig. 11).

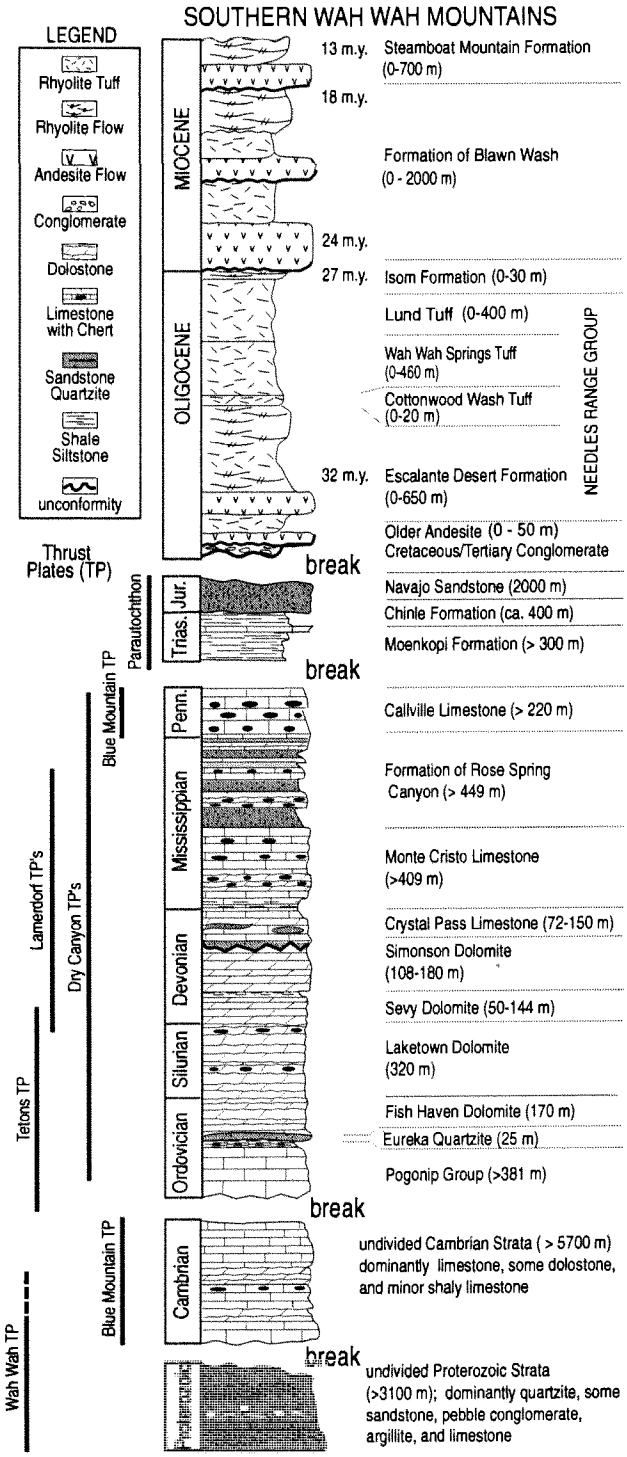

Figure 6. Generalized stratigraphic column for the southern Wah Wah Mountains. Late Proterozoic to Mesozoic strata are exposed in several thrust plates (TP's). For comparison with the Milford area, only the Paleozoic miogeoclinal and the Tertiary volcanic sections are shown in detail. Nomenclature of the units is after Abbott et al., (1983), Best and Grant (1987), and Best et al., (1987); unit thicknesses are from Hintze (1988) and Friedrich (1993). For more de- tailed descriptions of pre-Tertiary strata also see Miller (1966) and Weaver (1980).

gray, coarse- to medium-grained hornblende granodiorite, that is easily recognized by the presence of large (up to 1 cm), euhedral hornblende phenocrysts (Nielson et al., 1978; Sibbett and Nielson, 1980; Coleman, 1991). The porphyry of Lincoln Gulch in the southern Mineral Mountains (small map area of unit Ti1 southwest of exposures of the Cave Canyon detachment fault, fig. 2) is distinguished from this hornblende granodiorite by the presence of phenocrysts of biotite and K-feldspar, but is considered part of this intrusive episode on the basis of a preliminary U-Pb zircon age of approximately 23 Ma (D. S. Coleman, work in progress). Similarly, isolated outcrops of 23 Ma syenite in the Gillies Hill area and the Tushar Mountains are considered part of this intrusive episode (fig. 2; Steven et al., 1979; Cunningham et al., 1982). Locally the hornblende granodiorite was migmatized during intrusion of 18 Ma magmas (Stop 1-4; Coleman, 1991; Coleman and Walker, 1992). The presence of sphene in the migmatites is critical for field differentiation between Precambrian and Miocene gneiss: no dated Precambrian units contain sphene. At the northern end of the batholith the Oligocene granodiorite intrudes Cambrian carbonates, and on the western side it intrudes Precambrian wall rocks (Stop 1-5).

The vast majority of exposed plutonic rocks in the Mineral Mountains include coarse-grained, biotite-hornblende quartz monzonite, porphyritic quartz monzonite and granite that are extensively mixed with a coeval, dated 18.2 Ma (U-Pb zircon) diorite (Stop 1-3; Coleman, 1991; Coleman and Walker, 1992; Coleman et al., in preparation). Mixing of diorite and more silicic magmas is interpreted to have generated the variation of composition and texture in these units; therefore, they are considered together here and referred to as a the 'main intrusive phase'. Field relations indicate that the youngest pluton in the main intrusive phase is a 17.5 Ma (U-Pb zircon; Coleman et al., in preparation) leucocratic, garnet granite that crops out at the crest of the range and along the eastern margin of the batholith. Other small intrusive bodies including hornblende gabbro and syenite, and microgranophyric dikes (Condie, 1960; Nielson et al., 1978; Sibbett and Nielson, 1980) are included in the 18.2 to 17.5 Ma intrusive event on the basis of field relations with dated units (Coleman, 1991; Coleman et al., in preparation). Magmas of the main intrusive phase intruded Oligocene hornblende granodiorite on the northern side of the batholith, and Precambrian and Paleozoic rocks on the western and eastern sides (Stops 1-4, 1-5 and 2-1; Nielson et al., 1978; Sibbett and Nielson, 1980; Coleman, 1991).

The last intrusive episode recorded in the Mineral Mountains is widespread emplacement of porphyritic rhyolite and basalt dikes (fig. 2, included in unit Ti2; Stops 1-4, 1-5 and 2-1; Nielson et al., 1978; Sibbett and Nielson, 1980; Nielson et al., 1986; Coleman, 1991). This suite of 11 Ma

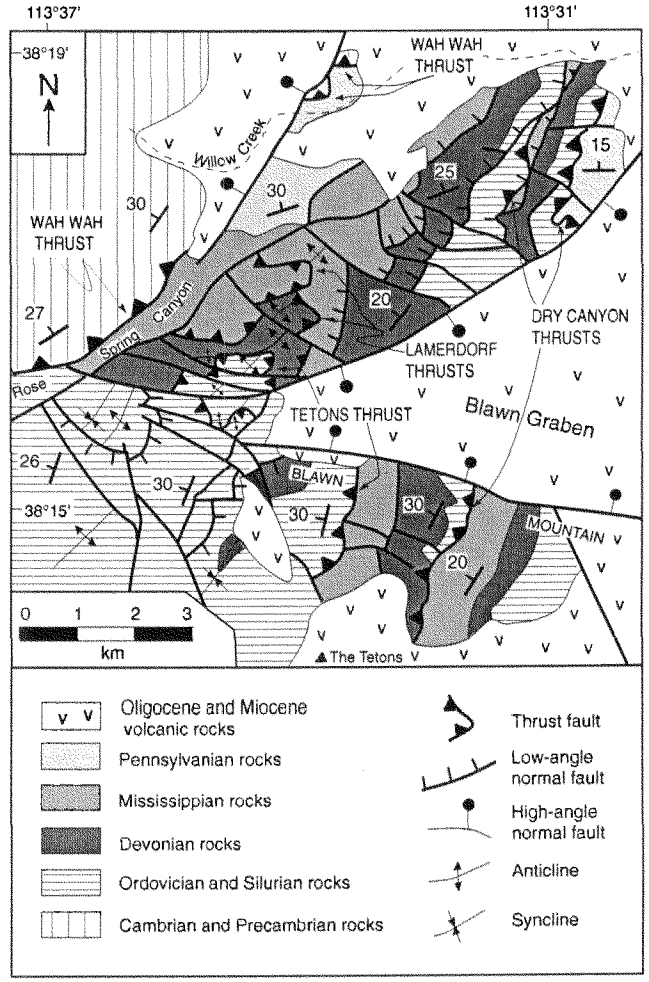

Figure 7. Simplified geologic map of the Rose Spring Canyon–Blawn Mountain area of the southern Wah Wah Mountains. See figure 14 for location. This figure shows the Wah Wah thrust and the backward-breaking imbricate thrusts in its footwall after Friedrich (1993). The Sevier thrusts and the oldest extensional faults are unconformably overlain by the basal volcanic rocks of the Oligocene Escalante Desert Formation.

(U-Pb zircon) dikes is correlative across the batholith and provides an important structural marker (Coleman and Walker, 1994). Although the dikes are mingled extensively, little mixing between the end members is evident.

Star Range. Rocks broadly resembling parts of the Mineral Mountains intrusive complex are exposed in small plutons scattered throughout the Star Range (fig. 2, unit Ti1; fig. 8). Their ages are not well established and, until these rocks are better studied, their relations to rocks in the Mineral Mountains remain unclear.

Three plutons or groups of plutons in the Star Range can be distinguished. A low spur extending from the east-central flank of the range is underlain by a relatively leucocratic

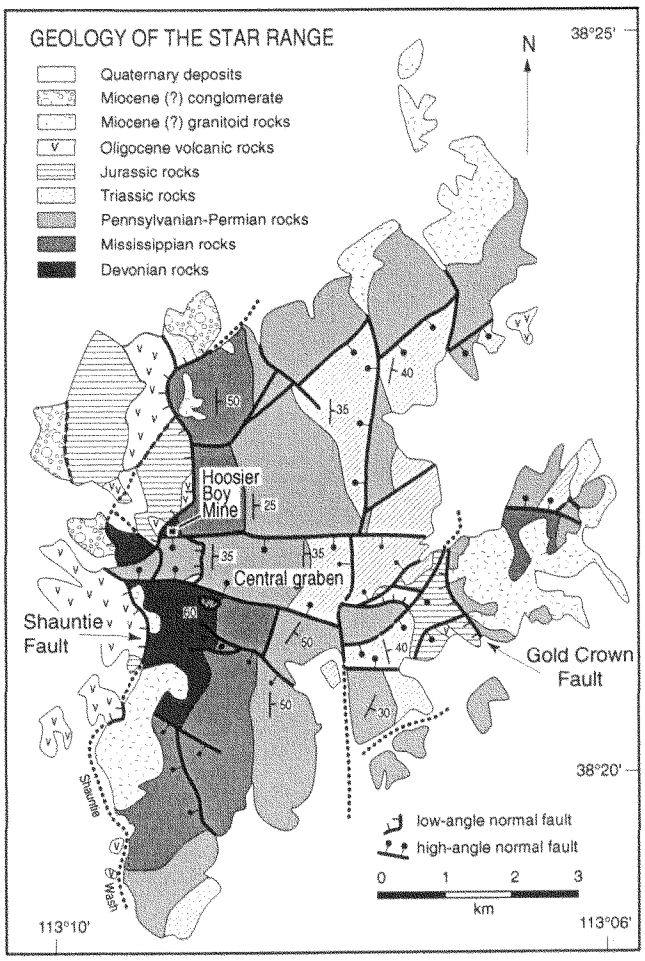

Figure 8. Geology of the Star Range simplified from Best et al., (1989a) and unpublished mapping by Bartley, Friedrich, Price and the 1990 University of Utah geology field class. Paleozoic-Mesozoic rocks that form the bulk of the range were interpreted to lie structurally above Mesozoic strata on the northwest flank along the Blue Mountain thrust. Our mapping indicates that the volcanic rocks deposited on these Mesozoic strata are juxtaposed with Paleozoic strata and the Miocene plutons that intrude them along a west-dipping, low angle normal fault (Shauntie fault). The Shauntie fault eliminates any need of, or evidence for, a thrust fault in the Star Range.

hornblende granodiorite pluton that intruded into upper Paleozoic and Triassic rocks. The exposures probably represent a cupola of a larger pluton that is continuous at depth because the intrusive contacts are highly irregular and rafts of wallrock are ubiquitous within the pluton. The northeastern third of the range provides exposures mainly of two plutonic rock types, porphyritic quartz monzonite which petrographically resembles the porphyry of Lincoln Gulch in the southern Mineral Mountains, containing large (up to 2 cm) K-feldspar phenocrysts, and mafic hornblende granodiorite to quartz diorite. Where exposed in mutual contact, these two rock types display clear magma-mixing textures. On the southwest flank of the range, a prominent leucogranite pluton forms the eastern wall of the canyon of Shauntie Wash. Early Miocene fission-track ages are reported from this pluton (Best et al., 1989b), but it is uncertain whether such ages record cooling after magmatic crystallization or later cooling related to unroofing.

Sedimentary Rocks

Mineral Mountains. Fine- to coarse-grained alluvium and colluvium occur throughout the Mineral Mountains. Alluvium generally comprises quartz and feldspar sand and gravel derived directly from weathering of the Tertiary plutonic units. Alluvium is apparently locally derived, and changes character (for example becomes darker near abundant diorite outcrop) with the locally dominant phase of the batholith.

Star Range. Some of the low hills on the west flank of the Star Range are underlain by a newly recognized Cenozoic rock unit that we informally call the conglomerate of the Hoosier Boy Mine (Stop 3-2). The hills had been mapped as Tertiary volcanic rocks (Best et al., 1989b) which is understandable because there are no outcrops and clasts in the float are mainly derived from the andesite of the Shauntie Hills. However, closer examination established the following points: (1) the clasts commonly are subangular to subrounded, indicating that they were transported from elsewhere rather than having weathered out of bedrock in situ; (2) although volcanic rocks predominate, clasts as large as 20 cm of fine-grained granitoid rocks are relatively common; (3) small clasts (< 8 cm) of Triassic sedimentary rocks, mainly red and green siltstone and fine-grained sandstone derived from the Chinle and Moenkopi formations, range from rare to moderately common. (4) Although immediately adjacent hills expose Paleozoic quartzite and carbonate rocks and Tertiary porphyritic quartz monzonite, no clast of these rock types has been found in areas underlain by the Hoosier Boy conglomerate. We interpret these observations to indicate that the Shauntie fault (see below) had not yet unroofed the adjacent Paleozoic and plutonic rocks when the Hoosier Boy conglomerate was deposited.

GEOLOGIC STRUCTURES

Geologic structures in the study area are typical of the Great Basin in that Mesozoic thrust faults are overprinted by Cenozoic extensional faults. Below we briefly summarize the structural geology in each of several areas we have studied in detail. Considerable emphasis is placed on the Mineral Mountains (including Antelope Mountain) which are the focus of this trip and where evidence for extensional

deformation and the timing relationship between extension and magmatism are well preserved.

Antelope Mountain

The principal structure on Antelope Mountain is the Antelope Mountain thrust (Stop 1-2; Liese, 1957; Whelan and Bowdler, 1979), which places Cambrian Prospect Mountain Quartzite over Cambrian Peasley/Dome Limestone and Cretaceous(?) conglomerate (fig. 4; Walker and Bartley, 1991). Although the actual thrust surface is not exposed, its location and attitude are tightly bracketed by outcrops. The thrust is folded into an open, east-plunging antiform. Tight folding of footwall rocks in the core of this antiform was synkinematic with contact metamorphism by the hornblende granodiorite intrusion and therefore we consider the folding to be related to emplacement of the Mineral Mountains batholith rather than to the Sevier orogeny.

The direction of emplacement of the Antelope Mountain thrust is uncertain, but its geometry is consistent with southeast vergence characteristic of the region. Footwall Cambrian rocks become stratigraphically higher to the south, but this relation is probably not related to ramping of the thrust because the intervening Cretaceous strata lie in angular unconformity on Cambrian footwall rocks. Thus, footwall rocks may have already dipped to the south before thrusting, and the footwall was deeply eroded by the time of deposition of the conglomerate. The cause of unroofing of the footwall probably was its elevation along a structurally lower thrust that we refer to as the sub-Antelope Mountain thrust. Considering the present distribution of the hanging wall, and assuming that the thrust climbs section at a moderate angle, displacement across the Antelope Mountain thrust must be at least 5 kilometers.

Tertiary structures at Antelope Mountain include map-scale folds and numerous moderate- to high-angle normal faults (fig. 4). The normal faults strike north or east and most have separations of tens to hundreds of meters. However, a north-striking fault zone on the western side of Antelope Mountain downdrops Middle Cambrian carbonate strata from the hanging wall of the Antelope Mountain thrust against footwall rocks (fig. 4, outcrops of Trippe(?) Limestone on far west side of Antelope Mountain). We know virtually nothing about either the Middle Cambrian stratigraphy or the internal structure of the Antelope Mountain thrust plate. Therefore, it is impossible to make a quantitative slip estimate for this fault zone.

Central Mineral Mountains

Because the central Mineral Mountains are underlain almost exclusively by massive granitoid plutons (fig. 2), the internal structure of this part of the range is difficult to recognize. Thin (less than 10 m) zones of cataclasite, ultracataclasite and mylonite which typically contain top-to-the-west shear-sense indicators are found throughout the main intrusive phase. The cataclastic-mylonitic foliation defines a broad north-south trending antiform across the range which Coleman (1991) interpreted to reflect folding of the range-forming block.

Range-scale folding is corroborated by structural orientations and paleomagnetic data from Paleozoic wallrocks and late Miocene dikes, and by the cooling history of the batholith. Rhyolite porphyry and basalt dikes in the northern (Stop 1-4) and western (Stop 1-5) Mineral Mountains consistently have nearly vertical dips and intrude nearly horizontal strata cut by nearly horizontal thrust faults. Dikes of the same swarm in the eastern part of the batholith (Stop 2-1) dip gently and intrude nearly vertical strata cut by nearly vertical thrust faults (Sibbett and Nielson, 1980; Coleman, 1991; Coleman and Walker, 1994). Paleomagnetism of the dikes and the rocks they intrude (both plutonic and wallrocks) supports the interpretation that the dikes were emplaced with subvertical dips and are variably tilted across the range up to a maximum of approximately 90° of west-side-up tilt on the east side of the range (fig. 9; Coleman et al., in preparation). Cooling dates ($^{40}Ar/^{39}Ar$ and fission-track) for the main intrusive phase are older on the east side of the batholith relative to those on the west side, consistent with rapid west-side-up tilt of the batholith after approximately 10 million years ago (Evans and Nielson, 1982; Coleman et al., in preparation).

Southern Mineral Mountains

The southern Mineral Mountains can be divided into three structural domains, from north to south: the Harkley Mountain domain, the Guyo graben, and the Yellow Mountain domain (fig. 10).

Harkley Mountain domain. The Harkley Mountain domain lies north of the Cherry Creek fault and includes exposures of the Cave Canyon detachment fault (fig. 11, map and section A-A′; Stop 2-2) which places steeply dipping upper Paleozoic rocks in its hanging wall upon the Mineral Mountains intrusive complex in the footwall (Nielson et al., 1986; Price, in preparation). Slip across the Cave Canyon detachment formed up to 100 meters of protocataclasite and cataclasite derived from footwall plutonic rocks. Extensional faulting and the intrusion of a small 11 Ma rhyolite porphyry pluton severely disrupted bedding in the hanging wall rocks.

Two adjacent fault surfaces mapped within the Harkley Mountain domain are interpreted to be eastern and western segments of the Cave Canyon detachment (fig. 11, section A-A′; Price, in preparation). The eastern segment undulates gently and the fault surface can be measured directly to be subhorizontal. The western segment dips 11° to 18°

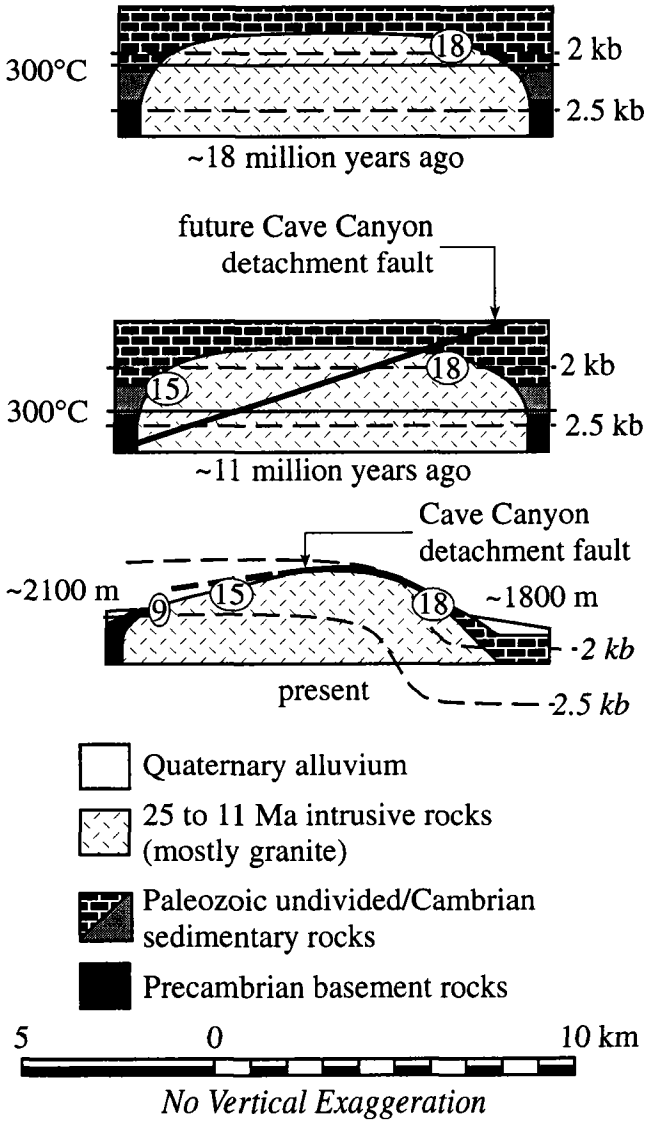

Figure 9. Cooling and deformational history of the Mineral Mountains batholith inferred from structural, thermochronologic and paleomagnetic data. Isobars are pressure estimates made using Al-in-hornblende barometry (Coleman, 1991). Numbers in white ellipses are biotite $^{40}Ar/^{39}Ar$ cooling dates in millions of years. We infer static cooling of the batholith between 18 and 11 Ma. By 18 Ma, the rocks of the main intrusive phase emplaced into Pennsylvanian strata had cooled below the 300°C isotherm. By 11 Ma, the 300°C isotherm had not reached the level where the batholith intrudes Proterozoic rocks. All of the exposed rocks had cooled below the 300°C isotherm by 9 Ma, following uplift and deformation of the batholith. Uplift was accompanied by tilting of the rocks on what is now the east side of the exposed batholith resulting in exposure of the shallowest levels of the batholith on the east and the deepest level of the batholith on the west. Uplifted and deformed isobars (indicated by italics) are shown in the last frame. Modified from Coleman et al., (in preparation).

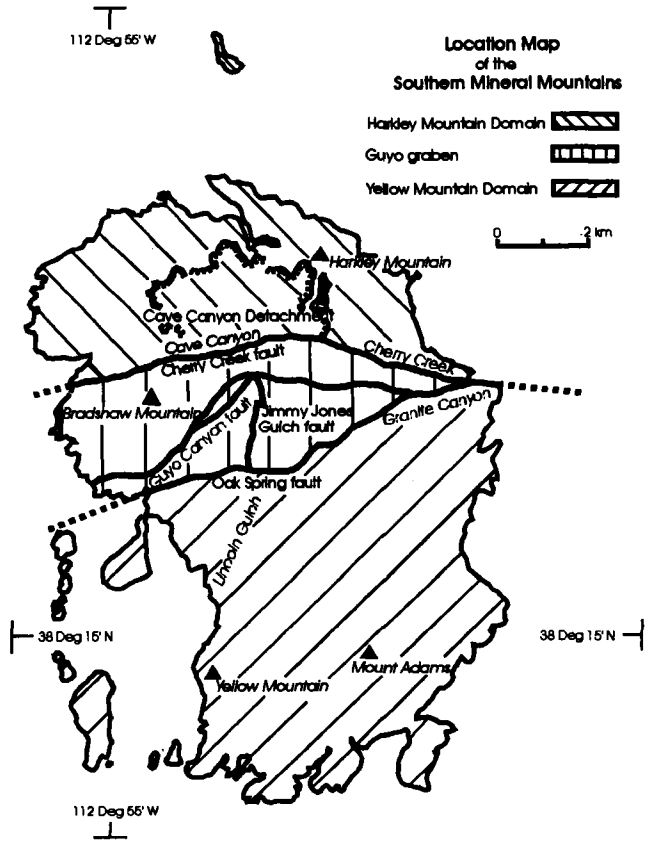

Figure 10. Structural domain map of the southern Mineral Mountains. See text for discussion.

west as determined by three-point solutions. Hanging wall rocks of the western segment were entirely removed by erosion such that the fault zone is recognized only as a layer of silicified cataclasite that caps a series of west-plunging ridges and is identical to that beneath the eastern segment. East- and north-striking high-angle faults cut both segments of the Cave Canyon detachment. Mapping did not reveal a direct spatial or temporal link between the two segments of the detachment fault (Price, in preparation).

Nielson et al., (1986) report that Tertiary rhyolite porphyry intrusions correlative with 11 Ma rhyolite porphyry dikes elsewhere in the Mineral Mountains (Coleman and Walker, 1994) cut the Cave Canyon detachment. However, detailed remapping revealed that the Cave Canyon detachment cuts all intrusive phases, including the Tertiary rhyolite porphyry, along its eastern segment. Whereas all earlier phases of the batholith are strongly cataclasized, however, the Tertiary rhyolite porphyry is scarcely deformed where it intrudes the cataclasite. This relation suggests that most of the displacement along the eastern segment of the detachment may have occurred before 11 Ma (Price and Bartley,

1992; Price, in preparation). Relations between Tertiary rhyolite dikes and the cataclasite along the western segment of the detachment are unknown.

Slip across the Cave Canyon detachment cannot be measured directly because no contacts or piercing points can be correlated from hanging wall to footwall. However, Paleozoic strata can be used to estimate the minimum separation. Wallrocks in the Beaver View Mine area (Stop 2-1) include dark dolomite lithologically resembling Devonian Simonson Dolomite, which is older than any rock currently exposed in the hanging wall of the Cave Canyon detachment in the Harkley Mountain domain. At least 9 kilometers of top-to-the-west slip across the Cave Canyon detachment is required to transport hanging wall Simonson Dolomite westward to a position stratigraphically below the younger hanging wall strata that are preserved (fig. 11, section B-B′; Price, in preparation).

Guyo graben. South of the Harkley Mountain domain is the east-west trending Guyo graben, which is defined by three broadly east-striking high-angle faults (the Cherry Creek, Oak Spring and Guyo Canyon faults) linked by several north- and northwest-striking faults (fig. 10). The northern margin of the graben is the Cherry Creek fault, an east-west striking, sub-vertical fault that places Paleozoic through Tertiary stratified rocks against both hanging wall and footwall rocks of the Cave Canyon detachment (fig. 11, map and section D-D′). The Oak Spring fault forms the southern margin of the Guyo graben and is interpreted to be non-planar and steeply dipping (fig. 11, section D-D′). Separation of rock units across the Oak Spring fault ranges from 300 to 600 meters down-on-the-north.

Running northeast to southwest within the Guyo graben is the non-planar south-dipping Guyo Canyon fault. This fault splays from the Cherry Creek fault near the eastern edge of the Mineral Mountains and converges with the Oak Spring fault at the western edge of the range. Dip separation across the Guyo Canyon fault is approximately 1500 to 1700 meters along much of its length. However, the fault rapidly loses separation in the western half of Guyo Canyon where it splays into several small faults. Many southwest-dipping faults cross from Guyo Canyon to Cave Canyon (fig. 11) and appear to transfer some of this displacement from the Guyo Canyon fault to the Cherry Creek fault. The remainder of the displacement is accommodated by a southeast-plunging fold east of Bradshaw Mountain.

Field relations between normal faults in the Guyo graben domain imply that all of the faults were active contemporaneously (Price, in preparation). The many small faults that splay off of the Guyo Canyon fault both cut and are cut by the north-south striking faults that link the Guyo Canyon fault to the Oak Spring fault. Nearly all of the north- and northeast-striking faults bridge between pairs of east-striking faults and do not cross them. Furthermore, there are no offset continuations of north-striking faults across the east-striking faults.

The location of the Cave Canyon detachment within the Guyo graben domain is uncertain. Its location depends on the nature of the Cherry Creek fault (fig. 12), which may represent a lateral ramp at which the Cave Canyon detachment either could step upward or downward, or it may be a younger fault that cuts and offsets the Cave Canyon detachment. It is also possible that the Cave Canyon detachment terminates at its southern end against the Cherry Creek fault and is not present in the Guyo graben domain (Price, in preparation). Present data do not permit confident selection between these alternatives, although the difficulty of matching rocks and structures across the Cherry Creek fault tends to argue against its interpretation as a younger fault.

Yellow Mountain domain. The Yellow Mountain domain extends from the Oak Spring fault on the north to Minersville Canyon on the south (fig. 10). The domain may be divided into three north-trending fault blocks defined by two inferred north-striking, west-dipping normal faults. However, the western and central blocks are exposed only in scattered low outcrops in the alluvial fan west of the range, and little is known about their structure because of poor exposure and low relief.

The eastern block of the Yellow Mountain domain forms the southern end of the Mineral Mountains and contains several interrelated sets of faults cutting Paleozoic through Tertiary strata. East-striking faults are linked with north-striking and predominantly west-dipping normal faults. The east-striking normal faults cut and offset the north-striking stratigraphic contacts and accommodate minor north-south extension (approximately 500 m, based on the cumulative heave of these faults in fig. 11, section D-D′). Neither east- or north-striking faults consistently cut the other, suggesting that, as in the Guyo graben, both fault sets were active at the same time (Price, in preparation).

Mapped north-striking faults in the Yellow Mountain domain repeat the Oligocene welded tuff sequence at the southern end of the range. These ash-flow tuffs terminate to the north against an east-striking fault north of Mt. Adams, here called the Mt. Adams fault (fig. 11). The outcrop width of andesite of the Shauntie Hills changes abruptly across this fault. The broad area underlain by andesite of the Shauntie Hills north of the Mt. Adams fault is unlikely to reflect an abrupt northward increase in stratigraphic thickness because the change occurs across a fault that equally affects the younger volcanic section. Therefore, cryptic west-dipping normal faults are hypothesized to repeat the andesite of the Shauntie Hills to the north of the Mt. Adams fault (fig. 11, Section C-C′). Thus, the Mt. Adams fault is interpreted to relay displacements between these two sets of north-striking domino-style normal faults.

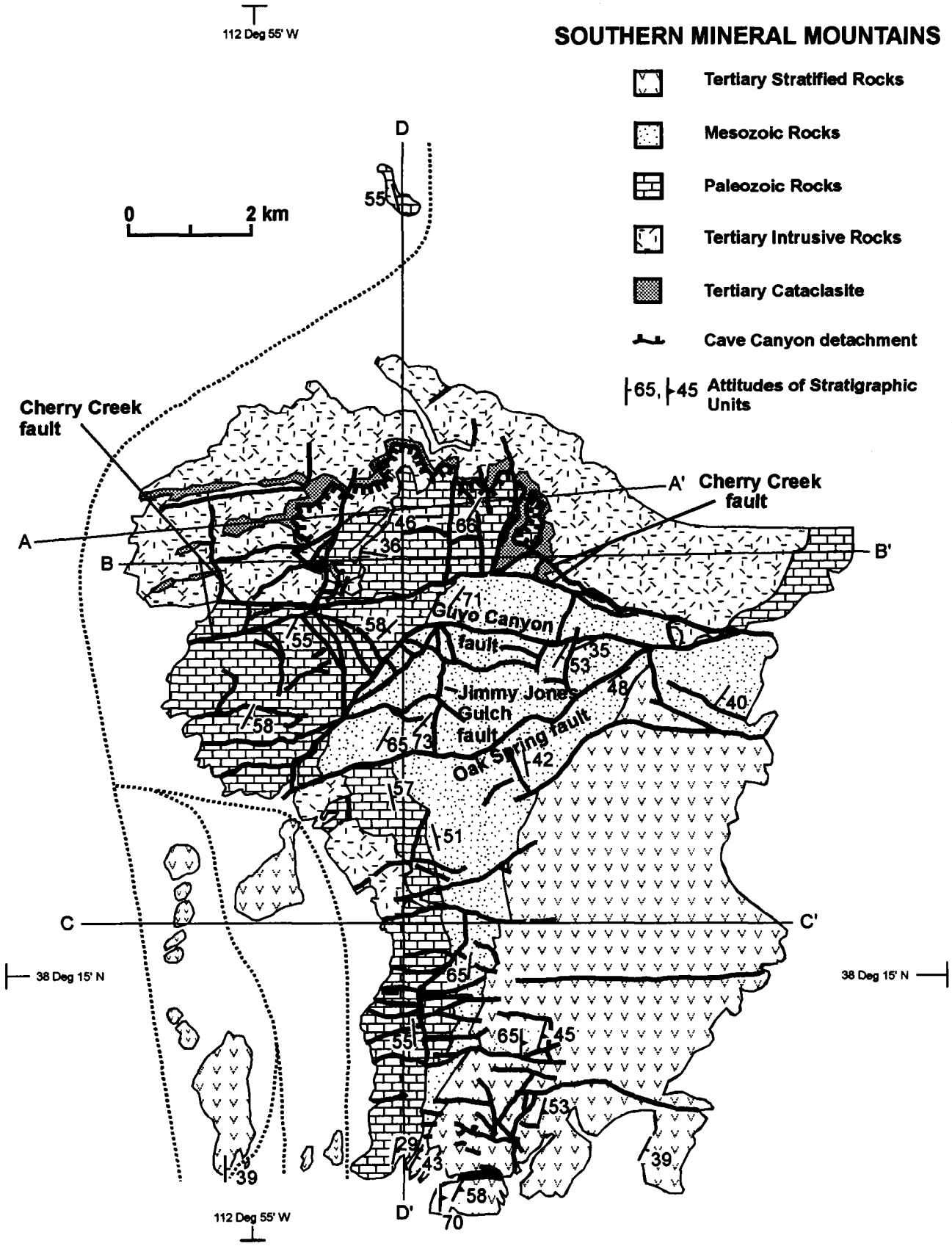
SOUTHERN MINERAL MOUNTAINS
Tertiary Stratified Rocks
Mesozoic Rocks
Paleozoic Rocks
Tertiary Intrusive Rocks
Tertiary Cataclasite
Cave Canyon detachment
65, 45 Attitudes of Stratigraphic Units
0 2 km
112 Deg 55' W
38 Deg 15' N
Cherry Creek fault
A
A'
B
B'
C
C'
D
D'
Guyo Canyon fault
Jimmy Jones Gulch fault
Oak Spring fault

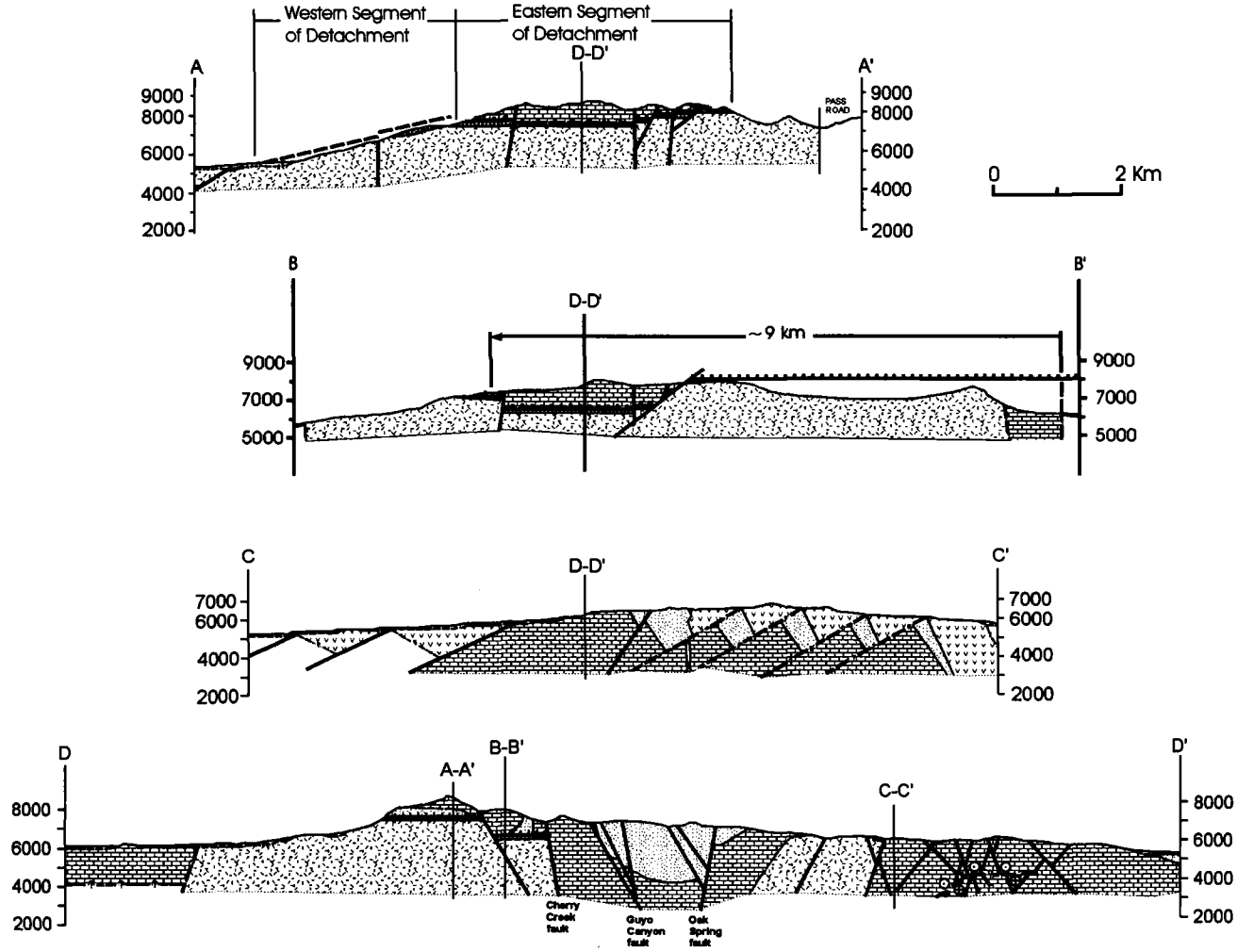

Figure 11. Simplified geologic map and cross-sections of the southern Mineral Mountains. Locations of cross sections are shown. Patterns on cross sections are the same as those shown on map. Mapping by D. Price.

The Yellow Mountain domain contains the only evidence in the area for pre-intrusive faulting. The 23 Ma porphyry of Lincoln Gulch cuts a west-dipping normal fault near the northeast corner of its exposure. Also, an angular unconformity between the three oldest ash-flow tuffs exposed in the southern Mineral Mountains (31 to 27 Ma) and the 26 Ma Isom Formation (Best and Grant, 1987) is suggested by a systematic dip discordance. Mean dips are 69° in the older ash-flow tuffs and 52° in the Isom Formation, whereas attitude data from individual fault blocks are discordant by from 9° to 25° (Stop 2-3). It is possible that the fault cut by the Lincoln porphyry reflects deformation related to tilting at 27 to 26 Ma, and may be related to the intrusion of the 25 ± 4 Ma granodiorite or collapse following eruption at 27 Ma of the Three Creeks tuff member of the Bullion Canyon Volcanics.

Faulting and tilting of the Tertiary section in the Yellow Mountain domain largely postdates the magmatic peak, however, and the amount of tilting varies throughout the domain. Tilting and erosion after deposition of the Tertiary Mt. Dutton Formation (approximately 21 Ma; Machette et al., 1984) formed a paleovalley in which quartz sandstone was deposited. Dip discordance indicates approximately 15° of eastward tilt between deposition of the Mt. Dutton Formation and the undated quartz sandstone. A basalt flow dated at 7.6 Ma (K-Ar whole-rock, Best et al., 1980) unconformably overlies the sandstone and dips 12° east (three-point solution on its basal contact). This indicates approximately 20 to 30° of further eastward tilt before 7.6 Ma and approximately 12° since 7.6 Ma. Bedding dips elsewhere in the domain record as little as 10° of tilt between 21 and 7.6 Ma and as much as 40° of tilt after 7.6 Ma.

Beaver Lake Mountains

The Beaver Lake thrust places Cambrian Prospect Mountain Quartzite on Mississippian Joana Limestone with two intervening horses of Cambrian rocks (fig. 13; Lemmon and Morris, 1984). Footwall rocks comprise Cambrian to Mississippian strata. The hanging wall consists of Prospect Mountain Quartzite passing up section into Dome Limestone. These rocks are probably in sequence with Cambrian-Ordovician Notch Peak Limestone exposed directly below the Frisco thrust in the adjacent San Francisco Mountains (fig. 1; Lemmon and Morris, 1984).

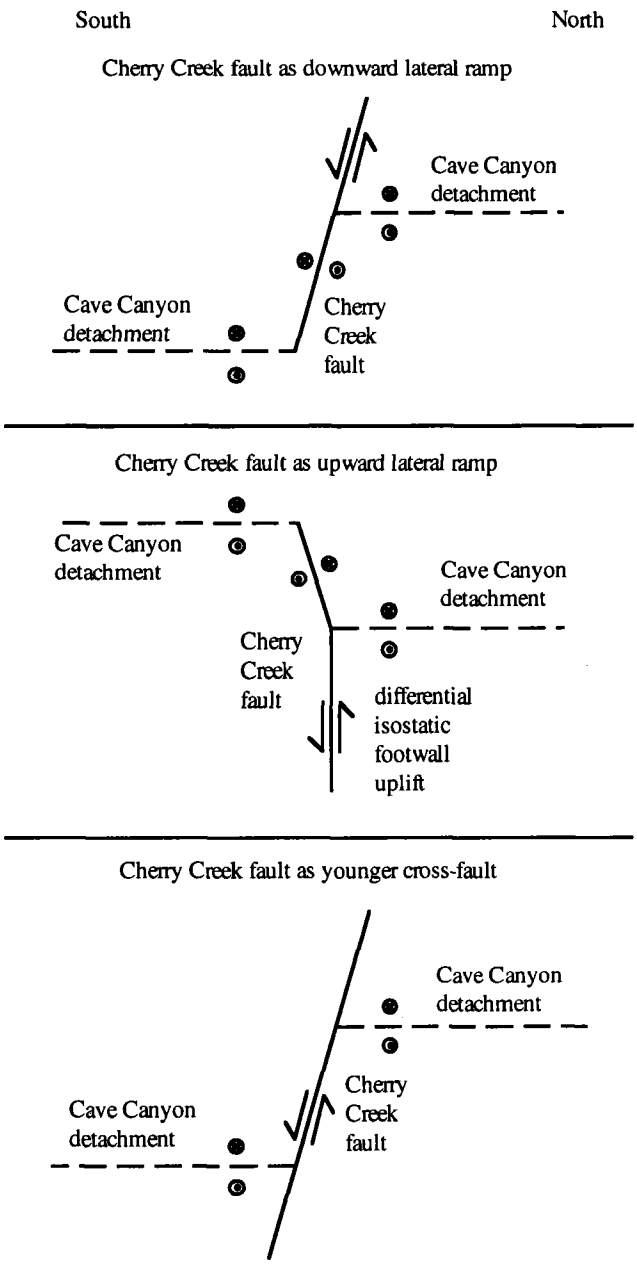

Figure 12. Possible geometries of the Cherry Creek fault as shown in simplified north-south cross sections approximately along the line D-D′ in figure 9. Arrows show direction of movement of the Cherry Creek fault (solid); circles with dots and X's show motion of the Cave Canyon detachment (dashed) out of, and into, the page, respectively. The first two frames show the Cherry Creek fault as a lateral ramp along the Cave Canyon detachment. We regard the second possibility (a south-side-up lateral ramp) as unlikely because the rocks exposed south of the Cherry Creek fault are unlike footwall rocks exposed elsewhere in the Mineral Mountains. However, the same basic geometry would result if the Cherry Creek fault is a tear fault that transfers the Cave Canyon detachment to the west. The final frame shows the Cherry Creek fault as a younger, cross-cutting, down-on-the-south structure. An additional possibility (not explicitly shown) is that the Cherry Creek fault is a tear fault that separates two distinct sets of fault blocks. In this case, the Cave Canyon detachment terminates against the Cherry Creek fault at its southern end. Existing data do not establish direction of motion across the Cherry Creek fault or the relative ages of the Cherry Creek fault and the Cave Canyon detachment. Therefore, we are unable to determine which of these possibilities is most likely.

The Beaver Lake Mountains are cut by numerous moderate- to high-angle Tertiary faults in widely varying orientations (fig. 13). The faults generally have small stratal separations. More significant Tertiary deformation is present, however, near the contact with the hornblende granodiorite (fig. 2, unit Ti1). Here, Paleozoic carbonate rocks are contact-metamorphosed to the point that a formation assignment is generally impossible, and contain a steep foliation subparallel to the intrusive contact. The contact aureole locally contains recognizable Middle Cambrian silty limestone that clearly is out of place relative to the Siluro-Devonian dolostones adjacent to the contact aureole. We interpret these Cambrian rocks to have reached their present position as a result of synmetamorphic shearing in the contact aureole. This steep structural zone corresponds directly to the steep southern limb of the Tertiary antiform adjacent to the same pluton on Antelope Mountain to the east across Milford Valley. This correlation suggests that shearing was pluton-side down and that the Cambrian rocks were derived from the Beaver Lake thrust sheet. Similar wallrock-pluton relations described elsewhere in the western United States are interpreted to result from sinking of plutons following a density increase associated with crystallization (Glazner, 1994; Glazner and Miller, 1996).

Star Range

The Star Range is composed of several fault-bounded blocks containing mainly east-dipping strata. Although faults of virtually every strike are present, four main faults define

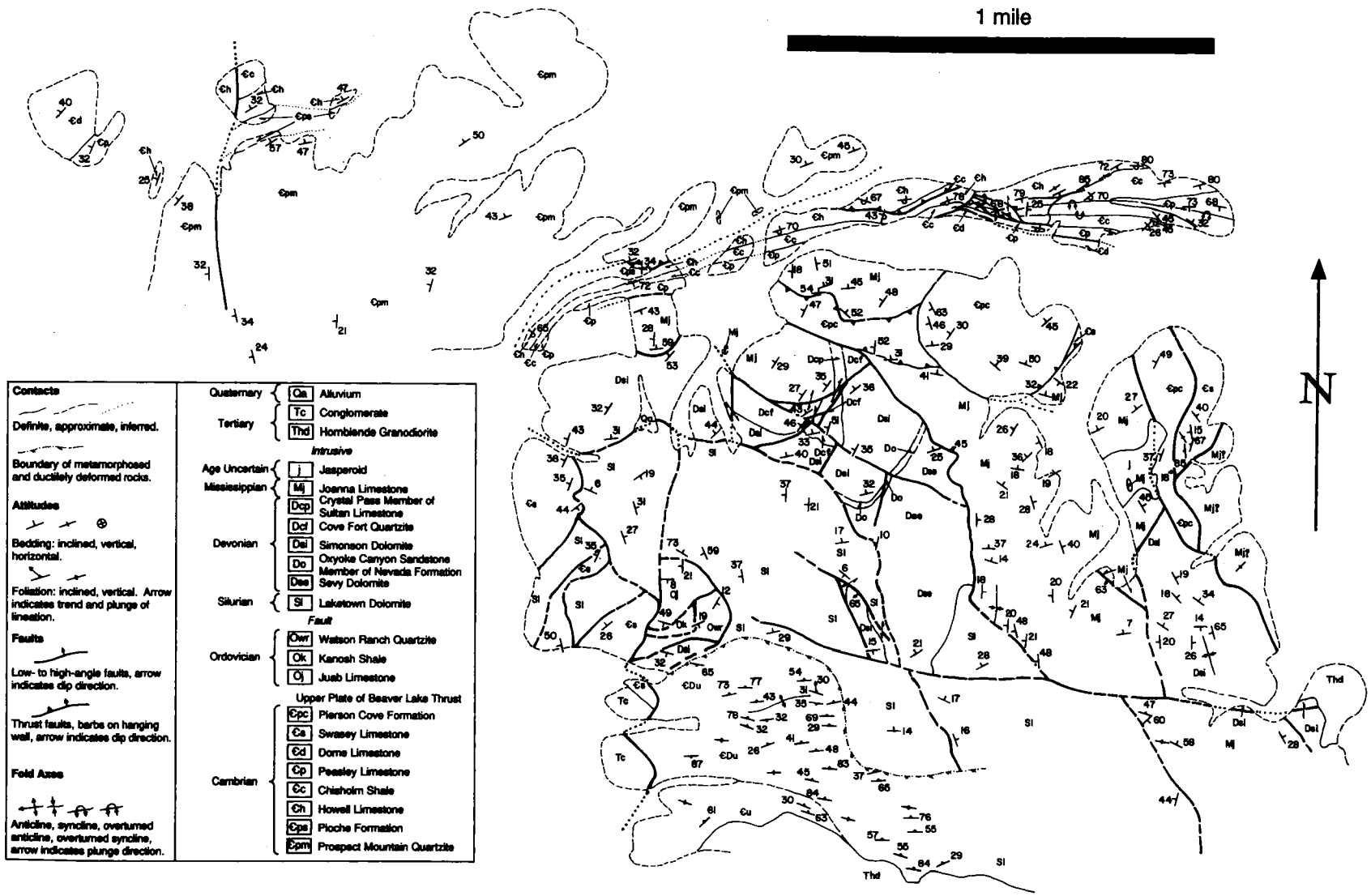

Figure 13. Geologic map of the Beaver Lake Mountain area. The Beaver Lake thrust and associated deformational features are well exposed in the northern part of the map area. Mapping by J.D. Walker and J.M. Bartley.

the overall structure. Two are west-dipping normal faults that we name the Shauntie fault and the Gold Crown fault, for mines located along their traces (figs. 2 and 8). The other two are east-striking normal faults that define what we call the Central graben.

The Shauntie fault is best exposed along Shauntie Wash (Stop 3-1), where it places a hanging wall of Jurassic Navajo Sandstone and 31 to 34 Ma andesite of the Shauntie Hills on the Miocene(?) Shauntie leucogranite pluton and its Paleozoic wallrocks. Horses of unmetamorphosed Paleozoic and Triassic sedimentary rocks are found locally along the fault, which dips 20 to 35° west. The fault was not recognized in previous mapping (Best et al., 1989b) but its presence is clearly demonstrated by (1) cataclasis along the contact and (2) the lack of contact metamorphism of rocks in the hanging wall adjacent to the leucogranite pluton, which has an extensive contact aureole elsewhere adjacent to its intrusive contacts.

A klippe of Mississippian rocks similar to that to be examined at Stop 3-1 rests on Devonian strata at the crest of the Star Range. The underlying fault dips very gently westward (approximately 5°). The klippe may represent a horse emplaced along a splay of the Shauntie fault, now isolated 1 kilometer from the main fault trace by erosion. This would imply that the overall dip of the Shauntie fault was quite low.

In the northwestern Star Range, Jurassic Navajo Sandstone and Oligocene Shauntie andesite are exposed across a narrow valley from Paleozoic carbonate rocks containing Tertiary granitoid intrusions. This relation matches that across the Shauntie fault but previously was interpreted to represent a window through the Blue Mountain thrust (Best et al., 1989b); that is, the alluvium was inferred to conceal an east-dipping thrust that emplaced the Paleozoic strata on the Navajo Sandstone. The andesite of the Shauntie Hills and Tertiary intrusions thus were interpreted to post-date juxtaposition of the Mesozoic and Paleozoic rocks. We reject this interpretation for at least four reasons.

1. The map pattern can be explained by continuing the Shauntie fault northward into this area. An unexposed thrust for which there is no other evidence therefore is not required.
2. Paleozoic rocks in the Star Range are relatively cratonal and resemble parautochthonous rocks in the southern Mineral Mountains. These rocks therefore are unlikely to have been carried above the Blue Mountain thrust which carries more miogeoclinal facies.
3. The andesite of the Shauntie Hills lies on the Navajo Sandstone along an irregular erosion surface as little as a few hundred meters from exposures of coarse-grained quartz monzonite intruded into Mississippian carbonate rocks. No intrusions are found on the west side of the valley and no volcanic rocks are found on the east side. This is a remarkable coincidence if juxtaposition of Paleozoic and Mesozoic rocks predated formation of any of the igneous rocks and the igneous rocks were emplaced in their present relative locations, as is required by the thrust interpretation.
4. The Hoosier Boy conglomerate was deposited on Tertiary volcanic and Mesozoic sedimentary rocks and mainly contains clasts derived from these units. It nowhere contains clasts of Paleozoic rocks, which in the thrust interpretation must have been exposed before Mesozoic rocks of the thrust window could have been. If the Paleozoic rocks structurally overlie the Mesozoic rocks, it is difficult to imagine how Paleozoic clasts could have been prevented from being incorporated in the Hoosier Boy conglomerate to which they are immediately adjacent.

Relations 3 and 4 are readily explained by the Shauntie normal fault. The hanging wall rocks were emplaced from an original location on the east side of the Star Range, providing suitable sources for the clast types in the Hoosier Boy conglomerate. Both the Paleozoic rocks and Tertiary intrusions in the western Star Range were unroofed by the Shauntie fault only after the plutons were emplaced in their Paleozoic wallrocks and after the Shauntie andesite and Hoosier Boy conglomerate were deposited. We therefore regard the entire Star Range to be composed of rocks that were parautochthonous relative to the Sevier fold-thrust belt.

The poorly exposed Gold Crown fault on the east side of the Star Range accomplished a very similar juxtaposition to the Shauntie fault. The hornblende granodiorite pluton on the east side of the range intruded and extensively contact metamorphosed Paleozoic and Triassic wallrocks, yet has an abrupt contact on its west side with unmetamorphosed Jurassic (and very locally Tertiary volcanic) strata. The geometry of the fault is not well defined by surface exposures, and the wall rocks of the pluton are highly faulted and can only locally be assigned to a particular formation. Therefore, the characteristics of the Gold Crown fault are less well determined than the Shauntie fault, but their mutual similarities suggest that they are part of a system of domino-style faults with similar slip magnitudes.

The main structure within the north-trending fault block between the Shauntie and Gold Crown faults is the Central graben, an east-trending graben bounded by nonrotational normal faults that dip toward each other at about 60° (fig. 8). The graben is roughly symmetrical with each bounding fault accommodating 1.0 to 1.5 kilometers of apparent throw, but apparent throw varies greatly along the graben owing to effects of intersecting faults both within the graben and

outside of it. The age of the Central graben cannot be determined directly. However, smaller east-striking normal faults subparallel to the southern bounding fault are cut by the Shauntie leucogranite pluton, which clearly is cut by the Shauntie fault. Therefore, we infer that the Central graben is older than the Shauntie fault.

Intersections of the Central graben with the Shauntie and Gold Crown faults are complex and incompletely understood. The simple graben geometry breaks down eastward into a plexus of variably oriented normal faults. Combined with the poor exposure of the Gold Crown fault itself, it is difficult to draw any clear conclusion about the chronology and kinematics of faults in this area. Relations at the westward intersection with the Shauntie fault are more clear-cut, however. Although the Central graben is believed to be older than the Shauntie fault, the Shauntie fault appears offset by the bounding faults of the Central graben (fig. 8). However, the sense of separation is the reverse of what would result if the Central graben cut the Shauntie fault: the Shauntie fault trace should be offset eastward, yet is offset to the west. We therefore interpret the offset to indicate that the bounding faults of the Central graben were propagation barriers to the Shauntie fault (e.g., Bartley et al., 1992), resulting in lateral stepping of the Shauntie fault and partial reactivation of the Central graben faults when the Shauntie fault intersected them.

Southern Wah Wah Mountains

The southern Wah Wah Mountains are the only area in western Utah where several Sevier thrust faults are exposed within a single range (figs. 7 and 14). Therefore, although the field trip makes no stops in the Wah Wah Mountains, they provide key insights into the geometrical evolution of the Sevier thrust system discussed here. The thrusts include the Blue Mountain thrust and the overlying Wah Wah thrust system, which comprises a complex imbricate thrust zone including, in ascending order in the nomenclature of Friedrich (1993), the Dry Canyon I and II thrusts, the Lamerdorf thrusts, the Tetons thrust, and the Wah Wah thrust (fig. 7).

The Wah Wah thrust is the largest-displacement thrust in southwestern Utah with minimum slip estimated by Friedrich (1993) at 38 kilometers. The Wah Wah and all other thrusts above the Dry Canyon I thrust each behead preexisting thrusts or thrust-related folds in their footwalls, implying that the Wah Wah thrust system is internally backward-breaking with structurally higher thrusts emplaced after lower ones. Final emplacement of the Wah Wah thrust, however, was followed by forward propagation of the main Sevier decollement to form a new frontal ramp at the Blue Mountain thrust (Fillmore, 1991).

The Sevier thrusts in the southern Wah Wah Mountains are cut by at least four sets of faults; the oldest and youngest fault sets have significant displacements and are discussed here (figs. 7 and 14). The oldest set of faults comprises southeast- and northwest-dipping low- to high-angle normal faults with a minimum cumulative heave of 650 meters (Friedrich, 1993; fig. 7). These faults are unconformably overlain by basal volcanic strata of the Oligocene Escalante Desert Formation and are the only known significant prevolcanic extensional faults in southwestern Utah (Friedrich and Bartley, 1992). The youngest fault set com-

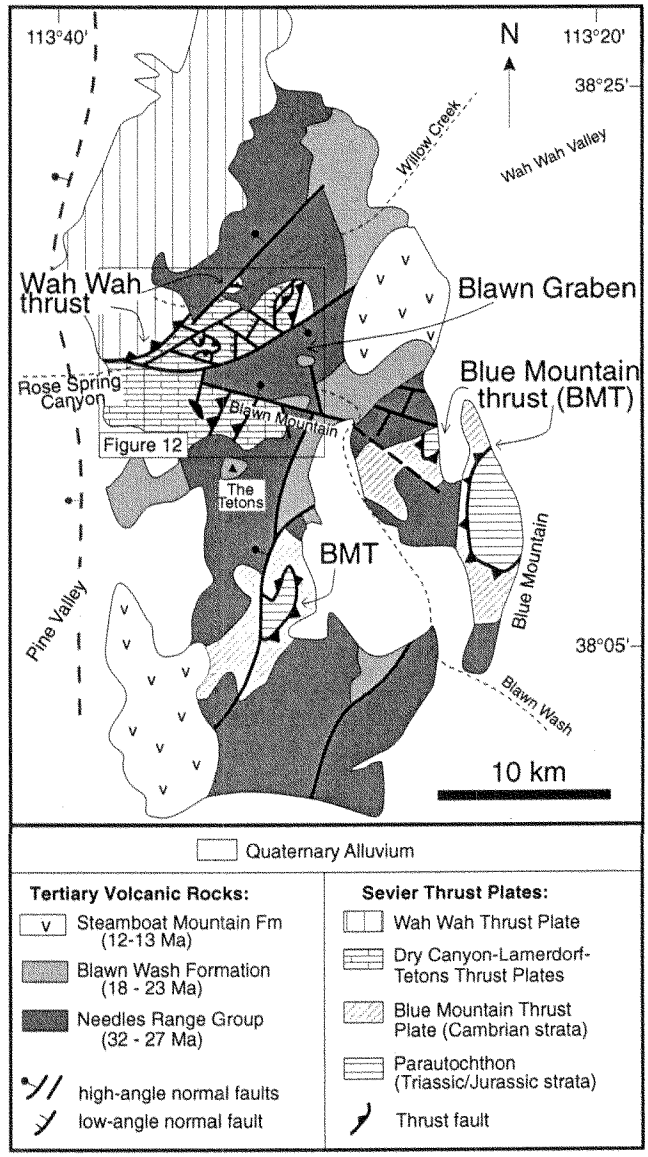

Figure 14. Tectonic map of the southern Wah Wah Mountains simplified from Weaver (1980), Abbott et al., (1983), Best et al., (1987b), and Friedrich (1993). This figure shows all levels of the frontal Sevier thrust belt and the timing relationships between extensional faulting and Oligocene to middle Miocene volcanism.

prises northeast- and east-striking high-angle normal faults of the Blawn graben which juxtapose volcanic rocks of the Miocene Blawn Formation against Paleozoic rocks with a stratigraphic separation increasing eastward from 300 meters to at least 1700 meters (figs. 7 and 14). The Blawn graben broadly geometrically resembles the Central graben of the Star Range and lies roughly on trend with it.

DISCUSSION AND CONCLUSIONS

There are four key questions we would like to address on this trip: (1) How are mapped thrust faults correlated across the Mineral Mountains region? (2) What is the regional relation between extension and magmatism? (3) What is the origin of low-angle extensional faults in the Mineral Mountains area? (4) What is the minimum amount of east-west directed extension in the Mineral Mountains area and how is this extension accommodated in the Sevier Desert to the north? We address each of these separately below.

Correlation of Mesozoic thrusts

The Wah Wah and Frisco thrusts were correlated by several previous workers (Miller, 1966; Armstrong, 1968; Morris, 1983; figs. 1 and 15). These thrusts form the base of the structurally highest major tectonic element in the Sevier thrust belt of western Utah, which is a regionally extensive allochthon of miogeoclinal strata that underlies most of the ranges of west-central Utah (fig. 15, Canyon Range-Wah Wah allochthon; Hintze, 1963, 1980; Armstrong, 1968). In the Wah Wah Mountains, an extremely complex imbricate stack underlies the Wah Wah thrust (fig. 7). We correlate the Beaver Lake thrust (fig. 13) with this zone of imbricate thrusts between the Pavant and Wah Wah thrusts on the basis of similarities in style, although older rocks are involved at the present level of exposure in the Beaver Lake Mountains. Continuation of the Blue Mountain thrust to the east is uncertain. It is not exposed in the Star Range which is interpreted to expose only parautochthonous strata (fig. 8). It may correlate with a possible thrust in the Rocky Range (fig. 2) because this thrust apparently juxtaposes Cambrian rocks with Triassic strata (Welsh, 1973).

We correlate the sub-Antelope Mountain thrust with the Beaver Lake thrust and Dry Canyon/Tetons thrust zone. This correlation is based on structural style and stratigraphy: at this position the thrust belt contains numerous imbrications and major horses. Our interpretation is consistent with correlation of the Antelope Mountain thrust with the Frisco/Wah Wah thrusts. These segments carry similar types of rocks and comprise the highest thrusts in these segments. We are unable to make a one-to-one correlation of the Blue Mountain, Dry Canyon, or Tetons thrusts. This difficulty is probably due to the tendency of these imbricate and complex faults to change character along strike.

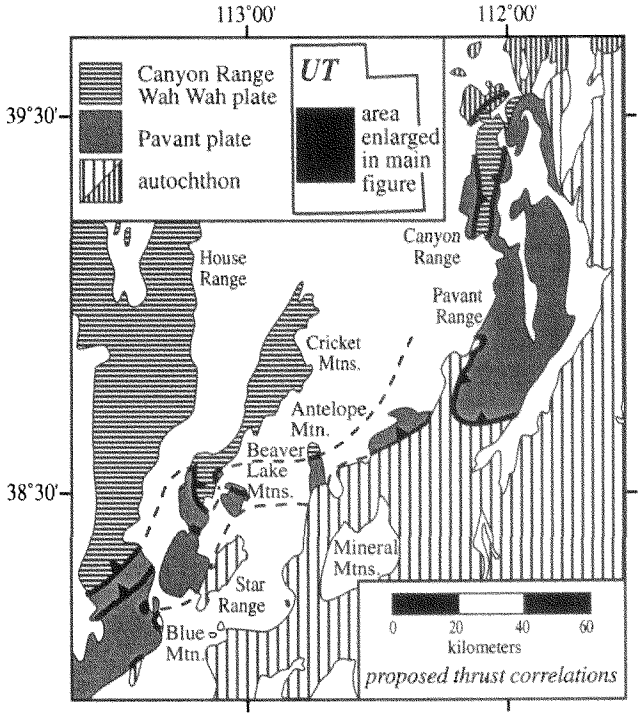

Figure 15. Correlation of thrusts and allochthons in the Milford area.

Correlation Between Extension and Magmatism

Extensional deformation in the Mineral Mountains area can be divided into north-south- and east-west-directed extension. Although mapping indicates that these two episodes of extension are partly contemporaneous in the southern Mineral Mountains, elsewhere in the area (as in the Basin and Range province in general [Axen et al., 1993]), development of east-trending grabens predates the main episode of north-striking Basin and Range faulting. Furthermore, throughout the area (and including the southern Mineral Mountains) development of north-trending detachment faults significantly post-dates the main period of magmatism.

It is tempting to interpret the east-trending grabens in the southern Mineral Mountains (Guyo graben; figs. 10 and 11), Star Range (Central graben; fig. 8) and Wah Wah Mountains (Blawn graben; fig. 14) to record a single event. In particular, tectonic models proposed by Bartley (1989) and Gans (1990), in which synmagmatic north-south extension is triggered by active spreading across the east-trending mid-Tertiary volcanic belt, predict such structures to have formed during the magmatic peak. However, timing relations in the study area do not consistently support this interpretation. The Central graben of the Star Range appears to date from before about 21 Ma and could have formed by

this mechanism. The Blawn graben, however, appears to be younger than 20 Ma although older than north-striking faults related to the main phase of Basin and Range extension (Friedrich, 1993). The Guyo graben in the southern Mineral Mountains appears to have developed contemporaneously with late Miocene north-striking normal faults (Price, in preparation). Although it is possible that the bounding faults of the Blawn and Guyo grabens were established earlier, there is no evidence that specifically suggests such an interpretation. The east-trending grabens thus have variable relations to regional magmatism and their tectonic significance remains obscure.

Evidence for ages of the large north-striking normal faults indicates that they are everywhere younger than early Miocene plutons. This is particularly clear in the case of the Mineral Mountains, where cross-cutting relations, thermochronology of lower-plate rocks, and paleomagnetic results combine to indicate that major extension began shortly before 11 Ma and mostly occurred after 11 Ma (Price and Bartley, 1992; Coleman and Walker, 1994; Coleman et al., in preparation; Price, in preparation). In contrast, the overwhelming majority of igneous rocks in the region formed in the period from about 32 Ma to 17 Ma. In the Star Range, cataclasis of rocks along the Shauntie fault and a lack of contact metamorphism across the fault indicate that the intrusive rocks had cooled significantly prior to deformation. Therefore, the main period of magmatism preceded the main period of crustal extension by several million years (Best and Christiansen, 1991), a relation that must be accommodated in physical models for crustal extension. For instance, it seems unlikely that Basin and Range extension in this area was either directly triggered or localized, or that trajectories of active faults were modified, by thermomechanical effects of the magmatism.

Origin of Presently Shallow Dips of Extensional Faults

The largest Cenozoic normal faults in the Mineral Mountains area strike north and dip to the west. Geometrical data concerning low-angle faults among this group consistently support their origins as steeper faults that were tilted to their present gentle dips by the isostatic rolling-hinge (Buck, 1988; Wernicke and Axen, 1988) or domino (Proffett, 1977) mechanisms. Locally, both isostatic rebound and tilting above structurally deeper faults may have contributed to the present geometry of faults.

The footwall to the Cave Canyon detachment preserves abundant evidence for deformation associated with isostatic rebound. Most notably, footwall rocks, deformation zones within footwall rocks and the Cave Canyon detachment are all folded in to a broad antiform across the Mineral Mountains (fig. 9). Maximum estimates of tilt are up to 90° on the far east side of the exposed batholith (Coleman and Walker, 1994; Coleman et al., in preparation). Price and Bartley (1992) and Price (in preparation) conclude that active segments of the Cave Canyon detachment were progressively abandoned as the footwall was tilted: currently active range-bounding faults on the far western side of the range dip steeply (Barker, 1986), whereas the western and eastern segments of the Cave Canyon detachment dip approximately 20° and 0°, respectively. Post-extensional tilting and isostatic uplift of the footwall block may have been localized by the Mineral Mountains batholith because there is no evidence for similar magnitudes of tilt at the breakaway zone for extension on the adjacent Colorado Plateau (Coleman et al., in preparation).

In addition to isostatic rebound, both the Cave Canyon detachment and other low-angle faults may have been, in part, tilted to their present orientation by domino-style normal faulting. Coleman and Walker (1994) concluded that up to 45° tilt of the Cave Canyon detachment and its footwall may have been accommodated by motion along the structurally deeper Beaver Valley fault (fig. 2). However, Price (in preparation) calls the existence of a separate Beaver Valley fault into question. Continued work in the region will help address these different interpretations. Regardless of the geometrical relations in the Mineral Mountains, we interpret the Shauntie and Gold Crown faults as a pair of domino-style faults.

The Magnitude of Regional Extension and Implications for Extension in the Sevier Desert

The absolute magnitude of extensional deformation across the Mineral Mountains region is difficult to measure due to limited exposure of hanging wall rocks and uncertainty in subsurface geology. However, it is possible to put broad minimum and maximum estimates on the amount of extension. Therefore, we frame this discussion in terms of limiting estimates: What is the bare minimum demanded by the geology? What is the maximum credible amount? Where in between these extremes is the real answer most likely to lie?

The minimum estimate for extension must account for (1) observed extension within ranges that did not contribute to forming the modern basins, and (2) formation of modern basins. Because the Cave Canyon detachment, Shauntie and Gold Crown faults do not appear to be correlative, displacements across them have to be additive. Separation across the Cave Canyon detachment is probably best understood and is at least 9 kilometers on the basis of restoring the Devonian Simonson Dolomite adjacent to correlative rocks in the footwall (Price, in preparation). This separation translates into an extension estimate of 4.5 to 8 kilometers assuming a fault with an initial dip of 60° to 30°, subsequently tilted to a horizontal orientation. Separation across

the Shauntie fault is less certain due to structural complications in the footwall and poor exposure of the hanging wall, but is approximately 4 to 5 kilometers based on separation of Jurassic strata across the fault. The Shauntie fault presently dips around 20° W and footwall strata dip about 40° E, indicating an initial fault dip of 60° and 40° of stratal tilt, which imply about 2 kilometers of extension. Because the juxtaposition of rocks across the Gold Crown fault is similar to that across the Shauntie fault (hanging wall of Navajo Sandstone and Tertiary volcanic rocks rests on a footwall composed of a Tertiary pluton intruded into Paleozoic carbonate rocks), we assume a similar amount of extension across the Gold Crown fault. Therefore, minimum extension across the ranges without opening any valleys is about 9 kilometers.

Estimates of minimum and maximum extension across the Beaver and Milford valleys are even more difficult to make than estimates of extension within adjacent ranges. To produce the observed basins in Beaver and Milford valleys, a bare minimum estimate of 1 kilometer extension across each is necessary assuming they are bounded by high-angle normal faults as shown by geophysical investigations (Smith and Bruhn, 1984; Barker, 1986).

A maximum estimate of extension across Beaver Valley (and part of the Mineral Mountains) is 10–15 kilometers on the basis of a match between a syenite/andesite (Ti1/Tmv) contact repeated across the Beaver Valley fault (fig. 2; Coleman, 1991). Walker and Bartley (1991) estimate a maximum of 30 kilometers of extension across Milford Valley on the basis of thrust correlations. This estimate is consistent with matching Tertiary intrusive/carbonate contacts (Ti1/CO-SD) between Antelope Mountain and the Beaver Lake Mountains (fig. 2). These estimates yield a minimum of about 11 kilometers and a maximum of about 40 kilometers of extension along a 40 kilometer line from the Colorado Plateau to the Shauntie Hills (the Shauntie Hills lie immediately west of the Shauntie fault on fig. 1).

The actual amount of extension across the Mineral Mountains region probably lies between these two extreme estimates. An approach to getting a somewhat less conservative minimum is to assume that faults similar to those exposed in the Mineral Mountains and Star Range exist under the adjacent valleys, too; we regard this as still conservative because the very existence of the valleys implies greater extension there than in the intervening ranges. The two ranges are each about 10 kilometers wide and each exposes one or more faults that accomplish 4 to 5 kilometers of extension. If the exposed faults represent a relatively uniform array of domino-style faults across the area, this implies 60 to 100% extension across a 40 kilometer transect, or 15 to 20 kilometers of total displacement. Assuming that the valleys exist because extension is more concentrated there than in the ranges, 20 kilometers of extension across the transect appears to be a reasonable minimum.

Any amount of extension between the Colorado Plateau and the Shauntie Hills must be either accommodated in the Sevier Desert along the Sevier Desert detachment to the north, or transferred to the west at the northern end of the Mineral Mountains along an unrecognized structure (fig. 1). Estimates of extension across the Sevier Desert detachment (20–60 kilometers; Allmendinger et al., 1983; Von Tish et al., 1985; Coogan and DeCelles, 1996) agree well with minimum and maximum estimates for extension in the Mineral Mountains region. This observation, combined with new data supporting extension in the Sevier Desert (Otton, 1995; Coogan and DeCelles, 1996, Linn et al., in review) and the lack of a suitable structure to transfer extensional deformation elsewhere, favor the interpretation that extension is accommodated within the Sevier Desert. Therefore, we favor the interpretation of the Sevier Desert reflector as a regionally significant detachment fault over other interpretations.

ROAD LOG

The road log starts in Beaver Utah each day of the trip. The reader is referred to figure 16 for a simplified road map of the field trip area.

START DAY 1

0.0	0.0	South Beaver entrance to I-15 at highway mile 109. Travel north. Look west to Mineral Mountains. Note high, craggy Granite Peak. Look east to Tushar Mountains.
3.1	3.1	Highway mile 112. North Beaver exit. Continue north.
8.9	12.0	Highway mile 120. Look northwest to Gillies Hill, east to Tushar Mountains.
2.5	14.5	Highway mile 123. Road cuts through Gillies Hill rhyolite
7.0	21.5	Highway Mile 130. Quaternary basalt flows west of I-15.
3.0	24.5	Highway mile 133. The Tushar Mountains are due east, Dog Valley lies to the north and the Pavant Range north of Dog Valley. Rocks in Dog Valley comprise an authochthonous Paleozoic section that is approximately horizontal. Allochthonous Paleozoic rocks crop out north of Dog Valley.
2.0	26.5	Exit 135 at historic Cove Fort.
0.1	26.6	Left on well graded Black Rock Road over I-15 continuing west. Low hills of Quaternary basalt.

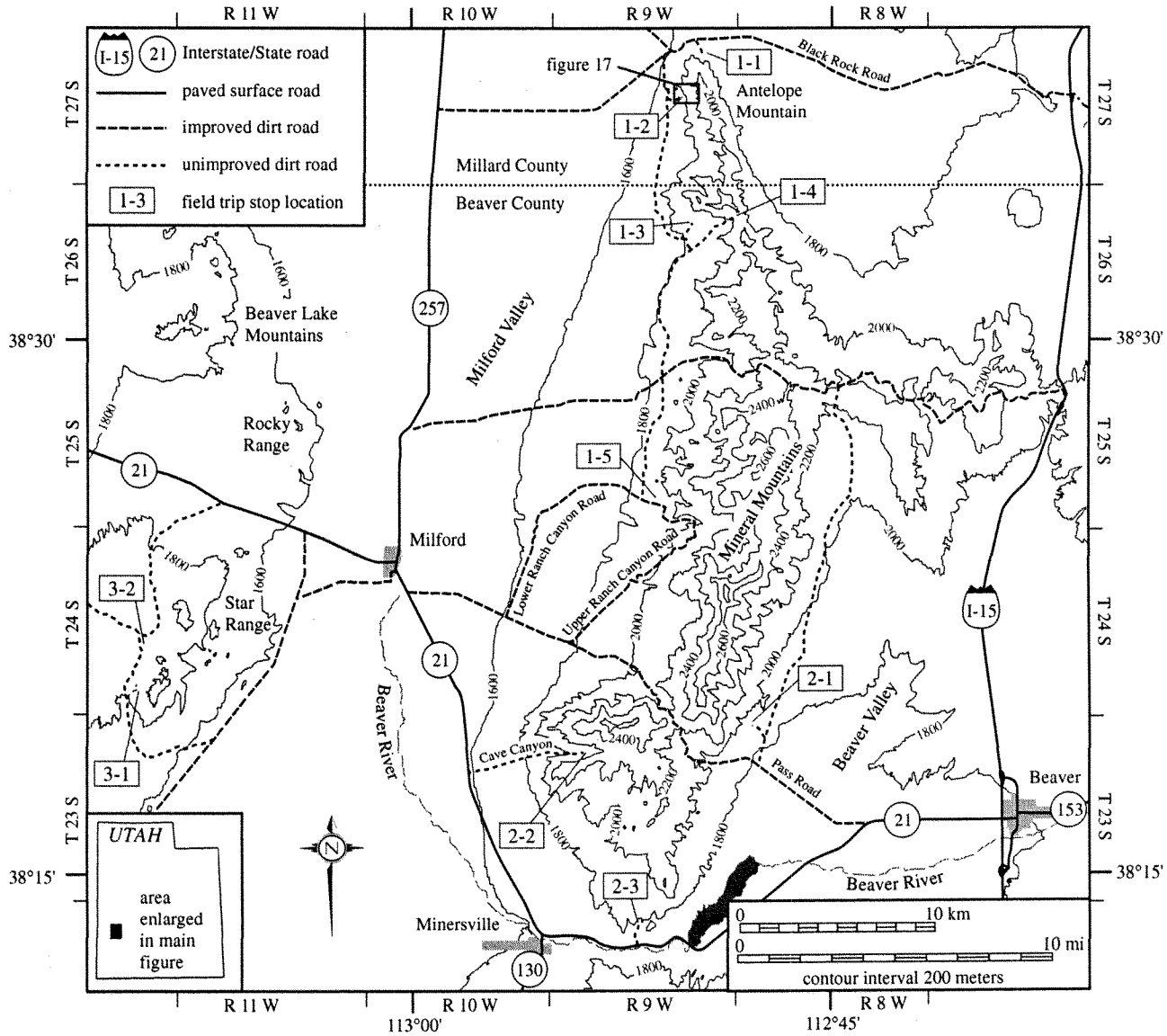

Figure 16. Road map for field trip. At many localities along the western side of the Mineral Mountains, there are complex intersections of unimproved dirt roads and it is recommended that you refer to appropriate U.S.G.S. 7.5 minute quadrangle maps. Topography and roads from U.S.G.S. Beaver, Wah Wah Mts. North and Wah Wah Mts. South 1:100 000, 30 X 60 minute quadrangle maps.

1.2	27.8	Cattle guard.
2.9	30.7	Cattle guard.
1.2	31.9	Top of hill. View to west-northwest is pass between Paleozoic section of Antelope Mountain to the north and plutons to the south. Note vertical dikes of rhyolite porphyry cutting plutonic rocks.
1.5	33.4	Fork, stay right.
1.2	34.6	Cattle guard.
5.4	40.0	Turn left on road at green gate and follow fence line.
0.5	40.5	**STOP 1-1. Overview of the Sevier Desert and the Beaver and Milford Valley area.** Park on float of the Prospect Mountain quartzite (fig. 4). Look north for a view of the Sevier Desert and the Canyon Range. The Cricket Mountains are to the northwest and the House Range is in the distant northwest. Here we have an overview of the Sevier Desert to the north. The Sevier Desert is underlain by a significant seismic reflector that is interpreted

variably as a detachment fault (e.g., Allmendinger et al., 1983; Von Tish et al., 1985) and an unconformity (Anders and Christie-Blick, 1994). According to the detachment model, the House Range and Cricket Mountains restore to a preextensional position 28 to 38 kilometers to the east of their current location (Sharp, 1984). The model of Anders and Christie-Blick (1994) predicts little or no offset across the Sevier Desert basin.

The view south is outcrop of Cambrian Prospect Mountain quartzite in the hanging wall of Antelope Mountain thrust. Looking to the south the Mineral Mountains are bounded by Beaver Valley to the east and Milford Valley to the west. Mapped faults and subsurface imaging of high-angle normal faults account for significant extension across the region. Our principal goal during this trip will be to examine the style of that extensional deformation and place some limits on the amount of extension. Somehow, that extension needs to be accommodated north of the Mineral Mountains. Two possibilities for this accommodation are an east-west trending strike slip fault zone or extension in the Sevier Desert.

0.5	41.0	Return to main road north of Antelope Mountain.
2.9	43.9	Take left fork toward Milford.
2.1	46.0	Left on road in small patch of sage and continue generally east toward range (this is a very tough intersection to find).
1.1	47.1	Gate through fence.
0.4	47.5	Left on road that continues east to the range.
0.6	48.1	**STOP 1-2. The Antelope Mountain thrust fault and underlying Cretaceous(?) conglomerate.**

Park where road gets bad, then walk up poor road and continue up wash to east-southeast (figs. 4 and 17). We will be walking up approximately 1000 feet through somewhat metamorphosed Cambrian Howell Limestone. The most altered rocks are at the start of the climb. The Antelope Mountain thrust fault is marked by the prominent ledge of Prospect Mountain Quartzite. Just below the quartzite are numerous exposures of conglomerate and siltstone presumably unconformably resting on the Howell Limestone. The relations at this stop indicate that the footwall rocks were uplifted, eroded down to the Howell Limestone, and subsequently overthrust by the Antelope Mountain thrust. The Antelope Mountain thrust fault has a consistently shallow-dipping orientation.

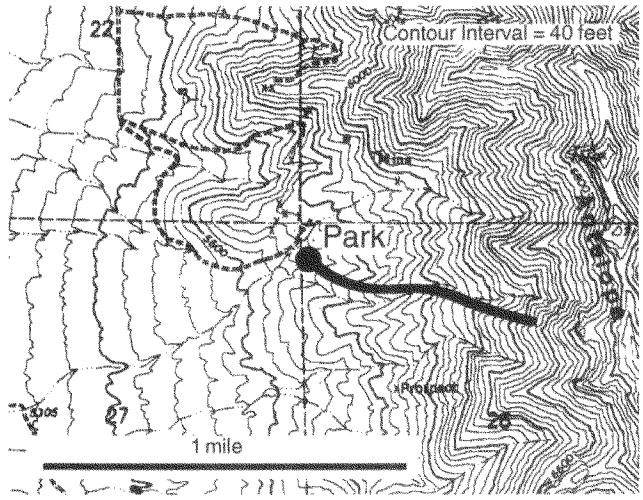

Figure 17. Topographic map showing exact location of outcrop for Stop 1-2.

0.6	48.7	Return to road and continue south.
0.5	49.2	Gate through fence.
2.0	51.2	Intersection with road on left. View east-southeast of spectacular mixed 18 Ma granite and diorite. Continue south along range front.
1.2	52.4	Left at T-intersection. In 50 feet turn hard to the right and continue south along the range front.
0.7	53.1	Bear left at fork.
0.4	53.5	Gate through fence. Immediately after gate take left on road to the north.
1.0	54.5	**OPTIONAL STOP 1-3. Magma mixing during the 18 Ma intrusive event.**

Park and walk west to outcrops of granite and diorite. Spectacular features resulting from mixing of magmas during the 18 Ma main intrusive event can be viewed on the hill past fence to the west. This mixing generates a regional variation in the composition of the diorite from diorite to granodiorite. The regional variation in the main intrusive phase composition

noted by Nielson et al., (1978) and Sibbett and Nielson (1980) from granite in the south to quartz monzonite in the north is also interpreted to result from this mixing event (Coleman, 1991). In addition to less modal quartz, the main intrusive phase has more abundant amphibole in areas where it is extensively mixed with the diorite. This variation is continuous across the batholith. Quartz xenocrysts with amphibole rims are abundant in the diorite and rapakivi feldspars are abundant in both phases in the mixing zones. Dikelets of granite in the diorite can be traced into zones of oriented and progressively randomly oriented feldspar xenocrysts. These observations provide an explanation for the common occurrence of K-feldspar "porphyroblasts" in mixed zones. All three magmatic events recorded in the Mineral Mountains pluton (25 Ma, 18 Ma and 11 Ma) are characterized by magma mixing or mingling.

1.0	55.5	Turn sharp left. Return to main road.
0.3	55.8	Left at fork.
0.6	56.4	Right at fork.
0.4	56.8	Turn left (green bus on right).
0.3	57.1	Bear left at fork down hill.
0.7	57.8	Bear right at fork.
0.1	57.9	Bear right at fork.
0.9	58.8	**STOP 1-4. Steeply-dipping 11 Ma rhyolite and basalt dikes in the northern Mineral Mountains.**

Park vehicles below Pinnacle Pass and climb to the top of the pass. Here we can view steeply dipping 11 Ma rhyolite porphyry dikes and a west dipping diorite dike in 18 Ma quartz monzonite. Paleomagnetism of these dikes and their wall rocks show minor, variable tilt from a Miocene expected direction (Coleman et al., in preparation). The geometric relations between rocks at the north end of the Mineral Mountains can be summarized as steeply dipping dikes intruding nearly horizontal strata cut by nearly horizontal thrust faults.

North of Pinnacle Pass, is the largest area of outcrop of 25 Ma intrusive rocks. At the north east end of Pinnacle Pass and along steep east facing cliffs continuing to the north are well-exposed Tertiary migmatites. Uranium-lead zircon geochronology of these migmatites reveals that they result from 18 Ma remobilization of 25 Ma hornblende granodiorite (Coleman, 1991).

0.9	59.7	Merge with road from right.
0.1	59.8	Merge with road from right.
0.7	60.5	Merge with road from left.
0.3	60.8	Major intersection, bear left (green bus on the right).
0.7	61.5	East side of road are commingled basalt-rhyolite dike intruding 18 Ma mixed granite-diorite pluton.
0.4	61.9	Cross road then turn right down northwest side of hill.
0.7	62.6	Merge with road from north.
0.6	63.2	Continue south at intersection.
0.6	63.8	Continue south at major intersection.
0.5	64.3	Ruins of the Negro Mag resort at the Roosevelt Hot Springs.
0.8	65.1	Right at Roosevelt Hot Springs, stay on the main road.
0.1	65.2	Cattle guard and intersection. Continue south.
0.4	65.6	Continue south.
0.3	65.9	Cross road and continue south. View to southwest is low white hill. This is the Opal Mound cut by the Opal Mound fault.
1.3	67.2	Cross road, continue south.
0.4	67.6	Bear left at fork.
0.1	67.7	Cattle guard.
1.0	68.7	Stay on main road bearing right after shallow wash.
0.8	69.5	Merge with road from northeast.
0.5	70.0	Sharp left onto well graded gravel road. (This is the Ranch Canyon loop road.)
0.6	70.6	**STOP 1-5. Steeply dipping 11 Ma dikes of the western Mineral Mountains and western wallrocks of the batholith.**

North of the Ranch Canyon loop, the low, northwest-trending ridge that ends in a low round hill includes outcrop of 11 Ma rhyolite porphyry dikes, 25 Ma hornblende granodiorite (along the low ridge) and 1725 Ma paragneiss (the round hill). Proterozoic rocks including paragneiss, sillimanite schist and quartzite comprise the western wall rocks of the batholith. Farther south, wallrocks also include Paleozoic marble. Note that rhyolite dikes along the western side of the batholith are

steeply dipping and yield Miocene expected paleomagnetic poles.

East of this stop, the batholith comprises well mixed diorite and granite of the 18 Ma intrusive event. To the south and east, Granite Peak (9580′ and the Milford Needle (9582′) expose 18 Ma granite, and are the highest points in the range. The high flat peaks immediately east of this location comprise Quaternary rhyolite lava domes. These are the source of the abundant obsidian float throughout the range. Geothermal activity at the Roosevelt Hot Springs, that we passed on the way to this location, attests to continued magmatic activity in the area.

0.6	71.2	Reverse direction. At intersection, continue toward Milford Valley on the Ranch Canyon Road.
1.1	72.3	Cattle guard.
6.7	79.0	Bear right toward Milford. This is the intersection with the Pass Road.
2.9	81.9	Cattle guard and start of pavement.
0.5	82.4	Turn left on Route 21 and return to Beaver (approximately 30 miles).

END DAY ONE

START DAY TWO

0.0	0.0	Start mileage at junction of highways 21 and 160. Continue west on 21 (Center Street) in downtown Beaver.
0.5	0.5	Underpass of I-15.
4.4	4.9	Exit right, and continue west on Pass Road into Mineral Mountains.
4.3	9.2	Turn right, and continue north along range front.
1.0	10.2	Turn left and continue west toward range.
0.5	10.7	**STOP 2-1. Steeply dipping wallrocks and horizontal 11 Ma dikes of the southeast part of the batholith.**

Park and proceed west on road over ridge. Walk to where road ends in wash and continue 100 meters up the wash to outcrops of Paleozoic carbonate and rhyolite porphyry. Climb to the top of the hill on the south side of the wash. The batholith here dominantly comprises 18 Ma quartz monzonite and granite, and 11 Ma rhyolite porphyry and basalt dikes. The dikes are correlative with vertical rhyolite porphyry and basalt dikes seen at Pinnacle Pass (Stop 1-3). The view to the south shows the steeply dipping carbonate rocks (Mississippian Redwall Limestone[?]/Devonian Simonson Dolomite[?]) that comprise the eastern wall rocks of the batholith. To the north, the carbonate rocks are cut by a (presently) steeply dipping thrust fault that is locally intruded by a rhyolite porphyry dike (Sibbett and Nielson, 1980). This is the only steeply dipping dike in this part of the Mineral Mountains (although it is difficult to discern the orientation of some dikes such as the one that caps this hill). Looking to the west, a basalt/rhyolite porphyry dike pair with near horizontal dips can be seen about three-quarters of the way up the side of the range. Horizontal rhyolite porphyry dikes are also evident above and west of the carbonate rocks looking south. The most accessible horizontal dikes crop out at the bottom of the wash we parked in, several kilometers west and up the side of the mountain. Paleomagnetic analysis of the horizontal dikes, the steeply dipping dike intruded along the fault, and the Paleozoic carbonate rocks all suggest that the rocks experienced up to 90i of west-side-up tilt (Coleman et al., in preparation). Thus, the dikes and the wall rock of the batholith are orthogonal to each other as they are at Pinnacle Pass; however, all are tilted approximately 90° relative to their orientations on the north and west sides of the batholith. We interpret this tilt to be the result of footwall uplift in response to denudation along the Cave Canyon detachment fault that we will examine at the next stop.

0.5	11.2	Turn around and proceed back to Pass Road. Turn right on range front road.
0.9	12.1	Bear right onto Pass Road (continuing west).
4.0	16.1	Road cut through dated 11 Ma rhyolite porphyry dike.
0.3	16.4	Cattle guard at Soldier's Pass.
3.5	19.9	Cattle guard.
1.4	21.3	Merge with Upper Ranch Canyon road. Continue down and to the west.
2.2	23.5	Merge with Lower Ranch Canyon road. Continue down and to the west.
3.0	26.5	Cattle guard and pavement begins.

0.5	27.0	Junction with Route 21, turn left continuing southeast toward Minersville.
6.5	33.5	Left onto Cave Canyon road. Road takes an immediate sharp right turn.
0.1	33.6	Cattle guard and road turns east toward range.
2.1	35.7	View of cataclasite capping hills north of the road.
0.5	36.2	**STOP 2-2. The Cave Canyon detachment fault.** Descend into Cave Canyon Wash and park. Walk approximately 1 mile east up Cave Canyon. The road starts in the canyon bottom, climbs onto the south slope, and then crosses back to the north slope just a little above the canyon bottom. When the road has crossed exposures of foliated granodiorite and rocks to the north have changed from intrusive rocks to Paleozoic carbonate rocks, look for the remains of a road on the left (difficult to find). Follow this road to the north approximately 0.5 mile and climb about 700 feet to the eastern end of cliff-forming outcrops with a subhorizontal top surface. The Cave Canyon detachment fault is exposed as the top surface of these cliffs (fig. 11 map and section A-A′). Paleozoic rocks in the hanging wall were transported a minimum of approximately 9 kilometers to the west. Proto-cataclasite and cataclasite are exposed in the cliff walls. Evidence of magma mixing can be seen within the proto-cataclasite. The cliffs terminate eastward against one of the late-stage, high-angle faults that cut the detachment. To the west, exposures of the cataclasite of the western segment of the detachment can be seen on the crests of west-plunging ridges. The Cherry Creek fault, exposed in the bottom of Cave Canyon, juxtaposes both the hanging wall and footwall rocks of the Cave Canyon detachment on the north against the Paleozoic through Tertiary stratified section to the south.
2.6	38.8	Reverse direction and return to route 21. Turn left continuing southeast toward Minersville.
5.9	44.7	Junction of 21 and 130 at Minersville, continue east toward Beaver.
3.2	47.9	Turn left off 21 on gravel road continuing north into low hills.
0.7	48.6	**STOP 2-3. Tilted rocks in the hanging wall of the Cave Canyon detachment fault.** Walk approximately 1.2 miles west (crossing a approximately 300′ high ridge) to the base of the volcanic section. A Cretaceous-Tertiary(?) conglomerate unconformably overlies the Triassic Moenkopi Formation at the sub-Tertiary unconformity. Walk eastward up-section through the volcanic units (fig. 5). The lower three ash-flow tuff units dip more steeply (approximately 70°) than the overlying Isom Formation (approximately 50°), although the amount of differential tilt varies between fault blocks. The traverse crosses an uninterrupted section into the Oligocene-Miocene Mount Dutton Formation, and then two fault blocks which repeat the section from the Three Creeks tuff member of the Bullion Canyon Volcanics to the Mount Dutton Formation.
0.7	49.3	Reverse direction and continue back to Route 21. Turn left on 21 continuing east toward Beaver.
2.8	52.1	Minersville State Park on left.
6.5	58.6	Pass Road junction, stay on 21.
4.4	63.0	I-15 underpass.
0.5	63.5	Junction of 21 and 160—main street of Beaver.

END DAY TWO

START DAY THREE

0.0	0.0	Start mileage at junction of highways 21 and 160. Continue west on 21 (Center Street) in downtown Beaver.
0.5	0.5	Underpass of I-15.
4.4	4.9	Junction with Pass Road.
6.5	11.4	Minersville State Park on right.
6.0	17.4	Junction 21 and 130 in Minersville. Stay on 21 toward Milford.
5.9	23.3	Junction with Cave Canyon Road. Continue on 21 northwest to Milford.
6.5	29.8	Junction with Pass Road. Continue on 21.
0.7	30.5	Railroad crossing. Bear right on 21 and immediately turn left on 500 S Street and continue to the west.
0.5	31.0	End of road, turn left continuing south.
0.4	31.4	Turn right at intersection just before pavement ends. Golf course on right.
0.3	31.7	Pavement ends.
0.7	32.4	Cattle guard.

0.4	32.8	Bear left at fork.
1.5	34.3	Bear left to follow powerline road.
1.4	35.7	Cattle guard.
1.9	37.6	Gold Crown mine west of road.
1.2	38.8	Cattle guard.
1.6	40.4	Leave powerline road, turn right on road continuing west to Star Range.
1.4	41.8	Cattle guard.
1.3	43.1	Fork, stay to right.
1.4	44.5	Fork, bear right.
0.7	45.2	**STOP 3-1. Geology of the Shauntie fault.** Stop between small hill (with klippe) and main range (fig. 8). Cross the wash and ascend the lower slopes of the reddish hill to the west. This hill is underlain mainly by altered and brecciated andesite of the Shauntie Hills, but its lower slopes on the east and south sides are Shauntie leucogranite. Ascending toward the contact, the leucogranite becomes progressively cataclasized, indicating that the contact is a fault rather than intrusive. This is the Shauntie fault, which is not well exposed here but dips about 30° west based on its intersection with topography. Return across the wash and ascend the slope to the south. Capping ridge are outcrops of dark gray Mississippian Monte Cristo Limestone. The limestone is shattered and silicified. The underlying leucogranite is again progressively cataclasized ascending toward the contact. Where the contact intersects a roadcut on the near side of the ridge, a zone of fault gouge several tens of centimeters thick is present. These relations are in stark contrast with intrusive contacts between the granite and limestone near the crest of the range, where the granite becomes vuggy and contains patches of pegmatite, and the dark limestone is bleached white and marmorized. We interpret the klippe here to be a horse along the Shauntie low-angle normal fault.
0.7	45.9	Reverse direction and return to last fork. Make a sharp right turn and continue north.
2.2	48.1	**STOP 3-2. Geology of the Shauntie fault and the Hoosier Boy conglomerate.** Top of pass with Hoosier Boy conglomerate. Shauntie fault and Central graben of the Star Range. The intersection of the Shauntie fault with the southern bounding fault of the Central graben is located near where the road turns left at the top of a steep hill and leaves the Shauntie Wash, heading west. The graben-bounding fault appears to be the younger than the Shauntie fault because it apparently truncates the Shauntie fault. However, as noted in the foregoing article, cross-cutting relations with the Shauntie leucogranite suggest the opposite age relation and the Shauntie fault here is offset in the incorrect sense for such an interpretation. Therefore, the trajectory of the Shauntie fault may have been deflected where it intersected the Central graben when propagating northward, here reactivating a short segment of the graben-bounding fault as part of the Shauntie fault.
0.3	48.4	Continue northward. At intersection turn right.
3.9	52.3	Bear right at fork.
2.4	54.7	Intersection with Route 21. Turn right and continue east toward Milford.
6.1	60.8	Main street, Milford. Right to return to Beaver, left to Salt Lake City.

ACKNOWLEDGMENTS

Supported by National Science Foundation grant EAR-8904007 to J. D. W. and EAR-8904329 awarded to J. M. B. and Geological Society of America and Sigma Xi grants to D. S. C. and D. E. P. and grants from CENEX and AAPG to D. E. P. Thanks to P. Price for assistance in data analysis and preparation of figures. The manuscript was greatly improved by reviews from Gary Axen, Myron Best, Paul Link and Gautam Mitra. We thank R.L. Bruhn and W.P. Nash for many helpful discussions, and S.E. Coleman for assistance in mapping and sample collection.

REFERENCES CITED

Abbott, J.T., Best, M.G., and Morris, H.T., 1983, Geologic map and cross sections of the Pine Grove-Blawn Mountain area, Beaver County, Utah: U.S. Geological Survey Miscellaneous Investigations Map I-1479, scale 1:24,000.

Aleinikoff, J.N., Nielson, D.L., Hedge, C.E., and Evans, S.H., 1987, Geochronology of Precambrian and Oligocene rocks in the Mineral Mountains, south-central Utah. U.S. Geological Survey Bulletin 1622, p. 1–12.

Allmendinger, R.W., Sharp, J.W., Von Tish, D., Serpa, L., Brown, L., Kaufman, S., and Oliver, J., 1983, Cenozoic and Mesozoic structure of the eastern Basin and Range province, Utah, from COCORP seismic-reflection data: v. 11, p. 532–536.

Anders, M.H., and Christie-Blick, N., 1994, Is the Sevier Desert reflection of west-central Utah a normal fault?. Geology, v. 22, p. 771–774.

Armstrong, R.L., 1968, Sevier orogenic belt in Nevada and Utah. Geological Society of America Bulletin, v. 79, p. 429–458.

Armstrong, F.C., and Oriel, S.S , 1965, Tectonic development of the Idaho-Wyoming thrust belt. American Association of Petroleum Geologists Bulletin, v 49, p. 1847–1866.

Axen, G.J., Taylor, W.J., and Bartley, J.M., 1993, Space-time patterns of the onset of extension and magmatism, southern Great Basin, Nevada, Utah, and California: Geological Society of America Bulletin, v. 105, p. 56–76.

Axen, G J., Bartley, J.M., and Selverstone, J., 1995, Structural expression of a rolling hinge in the footwall of the Brenner Line normal fault, eastern Alps. Tectonics, v. 14, p. 1380–1392.

Barker, C.A., 1986, Upper-crustal structure of the Milford Valley and Roosevelt Hot Springs, Utah region, by modeling of seismic refraction and reflection data [M.S. thesis]· University of Utah, 101 p

Barosh, P.J., 1960, Beaver Lake Mountains, Beaver County, Utah: Utah Geological and Mineral Survey Bulletin, v. 68, 89 pp.

Bartley, J.M., 1989, Changing Tertiary extension directions in the Dry Lake Valley area, Nevada, and a possible tectonic model, *in* Garside, L J , and Shaddrick, D.R., eds., Compressional and extensional structural styles in the northern Basin and Range. Nevada Petroleum Society, Seminar Proceedings, p. 35–39.

Bartley, J.M , Fletcher, J.M., and Glazner, A.F., 1990, Tertiary extension and contraction of lower-plate rocks in the central Mojave metamorphic core complex, southern California: Tectonics, v. 9, p. 521–534

Bartley, J M., Taylor, W.J., and Lux, D.R., 1992, Blue Ribbon volcanic rift in southeastern Nevada and its effects on Basin and Range fault segmentation· Geological Society of America Abstracts with Programs, v. 24, p. 2.

Best, M.G., McKee, E.H., and Damon, P.E., 1980, Space-time-composition pattern of late Cenozoic mafic volcanism, southwestern Utah and adjoining areas: American Journal of Science, v. 280, p. 1035–1050.

Best , M.G., and Grant, S.K., 1987, Stratigraphy of the volcanic Oligocene Needles Range Group in southwestern Utah and eastern Nevada. U.S. Geological Survey, Professional Paper 1433-A, p. 3–28.

Best, M.G., Mehnert, H.H., Keith, J.D., and Naeser, C.W., 1987, Oligocene and Miocene Volcanic Rocks in the central Pioche-Marysvale Igneous Belt, western Utah and eastern Nevada. U.S. Geological Survey, Professional Paper 1433-B, p. 29–47.

Best, M.G., Christiansen, E.C., and Blank, R H., Jr., 1989a, Oligocene caldera complex and calc-alkaline tuffs and lavas of the Indian Peak volcanic field, Nevada, Utah: Geological Society of America Bulletin, v. 101, p.,1076–1090

Best, M.G., Lemmon, D.W., and Morris, H.T., 1989b, Geologic map of the Milford Quadrangle and east half of the Frisco Quadrangle, Beaver County, Utah: U.S. Geological Survey, Miscellaneous Investigations, Map I-1904, scale 1.50,000.

Best, M.G., and Christiansen, E.H., 1991, Limited extension during peak Tertiary volcanism, Great Basin of Nevada and Utah. Journal of Geophysical Research, v. 96, p. 13509–13528.

Buck, R.W., 1988, Flexural rotation of normal faults· Tectonics, v. 7, p 959–973

Coleman, D.S., 1991, Geology of the Mineral Mountains Batholith, Utah [Ph.D thesis]. University of Kansas, 219 p.

Coleman, D.S., and Walker, J.D., 1992, Generation of juvenile granitic crust during continental extension. Journal of Geophysical Research, v. 92, p. 11011–11024.

Coleman, D.S., and Walker, J.D., 1994, Modes of tilting during extensional core complex development: Science, v. 263, p. 215–218

Coleman, D.S., Geissman, J.W., Walker, J.D., and Hodges, K.V., in preparation, Paleomagnetic and thermochronologic evidence for footwall tilt during extensional core complex development.

Condie, K.C., 1960, Petrogenesis of the Mineral Range Pluton, Southwestern Utah [MA thesis]: University of Utah, 99 p.

Coogan, J.C., and DeCelles, P.G., 1996, Extensional collapse along the Sevier Desert reflection, northern Sevier Desert Basin, western United States: Geology, v. 24, p. 933–936.

Crawford, A L., and Buranek, A.M., 1945, Tungsten deposits of the Mineral Range, Beaver County, Utah. Department of Mining and Metallurgical Research (University of Utah State Eng. Exp. Station) Bulletin, v. 25, 48 p.

Crecraft, H.R., Nash, W.P., and Evans, S.H., 1981, Late Cenozoic volcanism at Twin Peaks, Utah: Geology and petrology. Journal of Geophysical Research, v. 86, p. 10303–10320.

Cunningham, C.G., Ludwig, K.R., Naeser, C.W., Weiland, E.K., Mehnert, H.H., Steven, T.A., and Rasmussen, J.D., 1982, Geochronology of hydrothermal uranium deposits and associated igneous rocks in the eastern source area of the Mount Belknap volcanics, Marysvale, Utah. Economic Geology, v. 77, p. 453–463.

Davis, G.A., and Lister, G.S., 1988, Detachment faulting in continental extension; Perspectives from the Southwestern U.S. Cordillera, *in* Clark, S.P., Burchfiel, B.C., and Suppe, J., eds., Processes in Continental Lithospheric Deformation: Special Paper: Boulder, Geological Society of America Special Paper, p. 133–159

DeCelles, P.G., Lawton, T.F., and Mitra, G., 1995, Thrust timing, growth of structural culminations, and synorogenic sedimentation in the type Sevier orogenic belt, western United States: Geology, v 23, p. 699–702.

Earl, F.N , 1957, Geology of the Central Mineral Range [Ph.D. thesis]: University of Utah, 112 p.

Evans, S.H., and Nash, W.P., 1978, Quaternary rhyolite from the Mineral Mountains, Utah, U.S.A.: Salt Lake City, University of Utah, Department of Geology and Geophysics, 59 p.

Evans, S.H., and Nielson, D.L., 1982, Thermal and tectonic history of the Mineral Mountains intrusive complex: Geothermal Resources Council Transactions, v. 6, p. 15–18.

Evans, S.H., and Steven, T.A., 1982, Rhyolites in the Gillies Hill-Woodtick Hill area, Beaver County, Utah: Geological Society of America Bulletin, v. 93, p. 1131–1141

Fillmore, R.P., 1991, Tectonic influence on sedimentation in the southern Sevier foreland, Iron Spring Formation (Upper Cretaceous), southwestern Utah, *in* Nations, J.D., and Eaton, J.G., eds., Stratigraphy, depositional environments, and sedimentary tectonics of the western margin, Cretaceous Western Interior Seaway. Geological Society of America Memoir 260, p. 9–24.

Friedrich, A M., 1993, Analysis of the Mesozoic Wah Wah thrust system with Cenozoic extensional overprint, southwestern Utah [M S. thesis]: University of Utah, 112 p.

Friedrich, A.M., and Bartley, J.M., 1992, Geometry of the Wah Wah thrust zone, southern Wah Wah Mountains, SW Utah. Geological Society of America Abstracts with Programs, v. 24, p. 12.

Gans, P.B., 1987, An open-system, two-layer crustal stretching model for the eastern Great Basin. Tectonics, v. 6, p. 1–12.

Gans, P.B., 1990, Space-time patterns of Cenozoic N-S extension, N-S shortening, E-W extension, and magmatism in the Basin and Range province: Evidence for active rifting: Geological Society of America Abstracts with Programs, v. 22, p. 24.

Glazner, A.F., 1994, Foundering of mafic plutons and density stratification of continental crust. Geology, v. 22, p. 435–438.

Glazner, A.F., and Miller, D.M., 1996, Post-emplacement sinking of plutons: Geological Society of America Abstracts with Programs, v. 28, p. 69.

Heller, P.L , Bowdler, S.S., Chambers, H.P., Coogan, J.C., Hagen, E.S., Shuster, M.W., Winslow, N.S., and Lawton, T.F., 1986, Time of initial thrusting in the Sevier Orogenic belt, Idaho-Wyoming and Utah. v. 14, p. 388–391.

Hintze, L.F., 1963, Geologic map of southwestern Utah. Utah State Land Board, scale 1.250,000.

Hintze, L.F., 1974, Preliminary geologic map of the Wah Wah Summit quadrangle, Millard and Beaver Counties, Utah. United States Geological Survey Misc. Field Studies Map MF-637, scale 1.48,000

Hintze, L.F., 1980, Geologic map of Utah. Utah Geological and Mineral Survey, scale 1.500,000.

Hintze, L.F., 1988, Geologic History of Utah, Brigham Young University Geology Studies Special Publication 7, 202 p.

Hintze, L.F., and Robison, R.A., 1975, Middle Cambrian stratigraphy of the House, Wah Wah, and adjacent ranges in western Utah: Geological Society of America Bulletin, v. 86, p. 881–891.

Hoisch, T.D., and Simpson, C., 1993, Rise and tilt of metamorphic rocks in the lower plate of a detachment fault in the Funeral Mountains, Death Valley, California: Journal of Geophysical Research, v. 98, p. 6805–6827.

Holm, D.K., Geissman, J.W., and Lux, D.R., 1990, Paleomagnetic and Ar-Ar constraints on Tertiary uplift of the Black Mountains, Death Valley region, California. EOS, Transactions American Geophysical Union, v. 71, p. 1298.

John, B.E., and Foster, D.A., 1993, Structural and thermal constraints on the initiation angle of detachment faulting in the southern Basin and Range: The Chemehuevi Mountains case study. Geological Society of America Bulletin, v. 105, p. 1091–1108.

Lemmon, D.M., and Morris, H.T., 1984, Geologic map of the Beaver Lake Mountains Quadrangle, Millard and Beaver Counties, Utah. U.S. Geological Survey Map I-1572, scale 1.48,000.

Liese, H.C., 1957, Geology of the northern Mineral Range, Millard and Beaver counties, Utah [unpublished Master's thesis]: Salt Lake City, University of Utah, 88 pp.

Linn, J.K., Walker, J.D., and Stockli, D.F., in review, Timing of tectonic denudation of the Canyon Range, west-central Utah in response to footwall uplift of the Sevier Desert detachment. Geology.

Lipman, P.W., Rowley, P.D., Mehnert, H.H., Evans, S.H.J., Nash, W.P., and Brown, F.H., 1978, Pleistocene rhyolite of the Mineral Range, Utah. Geothermal and archaeological significance. United States Geological Survey Journal of Research, v. 6, p. 133–147.

Lister, G.S., and Baldwin, S.L., 1993, Plutonism and the origin of metamorphic core complexes. Geology, v. 21, p. 607–610.

Livaccari, R.F., Geissman, J.W., and Reynolds, S.J., 1993, Paleomagnetic evidence for large-magnitude, low-angle normal faulting in a metamorphic core complex. Nature, v. 361, p. 56–59.

Livaccari, R.F., Geissman, J.W., and Reynolds, S.J., 1995, Large-magnitude extensional deformation in the South Mountains metamorphic core complex, Arizona. Evaluation with paleomagnetism. Geological Society of America Bulletin, v. 8, p. 877–894.

Machette, M.N., Steven, T.A., Cunningham, C.G., and Anderson, J.J., 1984, Geologic map of the Beaver Quadrangle, Beaver and Piute Counties, Utah. U.S. Geological Survey, Miscellaneous Investigations, Map I-1520, scale 1:50,000.

MacDonald, R.E., 1976, Tertiary tectonics and sedimentary rocks along the transition. Basin and Range province to plateau and thrust belt province, Utah, *in* Hill, J.G., ed., Symposium on the Geology of the Cordilleran Hingeline. Denver, Rocky Mountain Association of Geologists, p. 281–317.

Manning, A.H., and Bartley, J.M., 1994, Postmylonitic deformation in the Raft River metamorphic core complex, northwestern Utah: Evidence of a rolling hinge. Tectonics, v. 13, p. 596–612.

Miller, G.M., 1966, Structure and stratigraphy of southern part of Wah Wah Mountains, southwest Utah. American Association of Petroleum Geologists Bulletin, v. 50, p. 858–900.

Morris, H.T., 1983, Interrelations of thrust and transcurrent faults in the central Sevier orogenic belt near Leamington, Utah. Geological Society of America, Memoir 157, p. 75–81.

Nash, W.P., 1976, Petrology of Quaternary volcanics of the Roosevelt KGRA, and adjoining area, Utah. Salt Lake City, University of Utah Publications Board, 102 p.

Nash, W.P., and Crecraft, H.R., 1982, Evolution of the Quaternary magmatic system, Mineral Mountains, Utah. Interpretations from chemical and experimental modeling, University of Utah, Department of Geology and Geophysics, 50 p.

Nielson, D.L., Sibbett, B.S., McKinney, D.B., Hulen, J.B., Moore, J.N., and Samberg, S.M., 1978, Geology of Roosevelt Hot Springs KGRA, Beaver County, Utah: Salt Lake City, Earth Science Laboratory, University of Utah Research Institute, 120 p.

Nielson, D.L., Evans, S.H., and Sibbett, B.S., 1986, Magmatic, structural, and hydrothermal evolution of the Mineral Mountains intrusive complex, Utah. Geological Society of America Bulletin, v. 97, p. 765–777.

Otton, J.K., 1995, Western frontal fault of the Canyon Range: Is it the breakaway zone of the Sevier Desert detachment?: Geology, v. 23, p. 547–550.

Parsons, T., and Thompson, G.A., 1993, Does magmatism influence low-angle normal faulting?. Geology, v. 21, p. 247–250.

Price, D.E., in preparation, Timing, magnitude, and three-dimensional structure of detachment-related extension, Mineral Mountains, Utah [M.S. thesis]: University of Utah.

Price, D.E., and Bartley, J.M., 1990, Low- and high-angle faulting, southern Mineral Mountains, southwestern Utah: Geological Society of America Abstracts with Programs, v. 22, p. 76.

Price, D.E., and Bartley, J.M., 1992, Three-dimensional extensional structure of the southern Mineral Mountains, southwestern Utah. Geological Society of America Rocky Mountain Section Abstracts with Programs, v. 24, p. 58.

Proffett, J.M.J., 1977, Cenozoic geology of the Yerington District, Nevada, and implications for the nature and origin of Basin and Range faulting. Geological Society of America Bulletin, v. 88, p. 247–266.

Reynolds, S.J., and Lister, G.S., 1990, Folding of mylonitic zones in Cordilleran metamorphic core complexes. Evidence from near the mylonitic front. Geology, v. 18, p. 216–219.

Reynolds, S.J., and Rehrig, W.A., 1980, Mid-Tertiary plutonism and mylonitization, South Mountains, central Arizona, *in* Crittenden, M.D.J., Coney, P.J., and Davis, G.H., eds., Cordilleran Metamorphic Core Complexes: Boulder, Geological Society of America Memoir 153, p. 159–175.

Royse, F., Jr., 1993, Case of the phantom foredeep. Early Cretaceous in west-central Utah. Geology, v. 21, p. 133–136.

Scott, R.J., and Lister, G.S., 1992, Detachment faults. Evidence for a low-angle origin: Geology, v. 20, p. 833–836.

Sharp, J.W., 1984, West-central Utah: palinspastically restored sections constrained by COCORP seismic reflection data [M.S. thesis]. Cornell University, 60 p.

Sibbett, B.S., and Nielson, D.L., 1980, Geology of the central Mineral Mountains, Beaver County, Utah. Salt Lake City, Utah University Research Institute, Earth Sciences Laboratory Report no. 33, 42 p.

Smith, R.B., and Bruhn, R.L., 1984, Intraplate extensional tectonics of the eastern Basin-Range: inferences on structural style from seismic reflection data, regional tectonics, and thermal-mechanical models of brittle-ductile deformation. Journal of Geophysical Research, v. 89, p. 5733–5762.

Steven, T.A., Cunningham, C.G., Naeser, C.W., and Menhert, H.H., 1979, Revised stratigraphy and radiometric ages of volcanic rocks and mineral deposits in the Marysvale area, west-central Utah. 40 p.

Von Tish, D.B., Allmendinger, R.W., and Sharp, J.W., 1985, History of Cenozoic extension in central Sevier Desert, west-central Utah, from COCORP seismic reflection data. American Association of Petroleum Geologists Bulletin, v. 69, p. 1077–1087.

Walker, J.D., and Bartley, J.M., 1991, New thrust fault relations in the Beaver Lake Mountains, southwestern Utah, and regional correlation

of Sevier thrusts: Geological Society of America Abstracts with Programs, v. 23, p. 107.

Walker, J.D., Bartley, J.M., and Glazner, A.F., 1990, Large-magnitude extension in the central Mojave Desert. Implications for Paleozoic to Tertiary paleogeography and tectonics. Journal of Geophysical Research, v. 95, p. 557–569.

Weaver, C.L., 1980, Geology of the Blue Mountain Quadrangle, Beaver and Iron Counties, Utah: Brigham Young University Geology Studies, v. 27, p. 116–132.

Welsh, J.E., 1973, Geology of the Beaver Lake Mountains, Beaver County, Utah· Utah Geological Association Publication 3, p. 49–53.

Whelan, J., and Bowdler, J., 1979, Geology of the Antelope Springs quadrangle Millard County, Utah: Utah Geology, v. 6, p. 81–85.

Wernicke, B., 1981, Low-angle normal faults in the Basin and Range Province· Nappe tectonics in an extending orogen: Nature, v. 291, p. 645–648.

Wernicke, B P., and Axen, G.J., 1988, On the role of isostasy in the evolution of normal fault systems: Geology, v. 19, p. 848–851.

Wright, J.E., and Snoke, A.W., 1993, Tertiary magmatism and mylonitization in the Ruby-East Humbolt metamorphic core complex, northeastern Nevada: U-Pb geochronology and Sr, Nd, and Pb isotope geochemistry. Geological Society of America Bulletin, v. 105, p. 935–952